Magnesium ferrite/ activated carbon ($MgFe_2O_4$/ AC) composite for simultaneous removal of Ni (II), Co (II), Cd (II) and Cu (II) from wastewater via adsorption

Subul Huda
Registration No: 02312013015

DEPARTMENT OF ENVIRONMENTAL SCIENCE
FACULTY OF BIOLOGICAL SCIENCES
QUAID-I-AZAM UNIVERSITY
ISLAMABAD, PAKISTAN
2020-2022

Magnesium ferrite/ activated carbon ($MgFe_2O_4$/ AC) composite for simultaneous removal of Ni (II), Co (II), Cd (II) and Cu (II) from wastewater via adsorption

A dissertation submitted in partial fulfillment of the requirement for the degree of

Master Of Philosophy

In

Environmental Sciences

Subul Huda

Registration No: 02312013015

DEPARTMENT OF ENVIRONMENTAL SCIENCE

FACULTY OF BIOLOGICAL SCIENCES

QUAID-I-AZAM UNIVERSITY

ISLAMABAD, PAKISTAN

2020-2022

PLAGIARISM UNDERTAKING

I, Subul Huda (Registration No**.** 02312013015.), hereby state that my M.Phil. Thesis titled "**Magnesium ferrite/ activated carbon ($MgFe_2O_4$/ AC) composite for simultaneous removal of Ni (II), Co (II), Cd (II) and Cu (II) from wastewater via adsorption**" is solely my research work with no significant contribution from any other person. Small contribution/help whatever taken has been duly acknowledged and complete thesis has been written by me.

I understand zero tolerance policy of the HEC and Quaid-I-Azam University, Islamabad, towards plagiarism. Therefore, I as an author of the above titled thesis declare that no portion of my thesis has been plagiarized and a reference is properly referred /cited for any material used.

I undertake that if I am found guilty of any form of plagiarism in the above tilted thesis even after the award of M.Phil. degree, the university reserves the right to withdraw/revoke my M.Phil. degree and that HEC and the university has the right to publish my name on the HEC/University website on which the names of students are placed who submitted plagiarism.

Subul Huda

AUTHOR'S DECLARATION

I, Subul Huda (Registration No. 02312013015), hereby state that my M.Phil. thesis titled as "**Magnesium ferrite/ activated carbon ($MgFe_2O_4$/ AC) composite for simultaneous removal of Ni (II), Co (II), Cd (II) and Cu (II) from wastewater via adsorption**" was carried out by me in the Renewable Energy Advancement Laboratory, Department of Environmental Sciences, Quaid-I-Azam University, Islamabad. The results, findings, conclusions, and investigations of this research have not been previously presented and have not been published as a research work in any other university.

Subul Huda

Table of Contents

ACKNOWLEDGEMENT

I am very grateful to Allah Almighty, who is the most merciful and beneficent, who has blessed me with all his blessings and helped me and gave me strength to carry out this dissertation work.

I am fortunate that I had the supervision of **Dr Abdullah Khan,** who has helped and encouraged me throughout with his guidance, and support. I would like to pay my sincere regards for his exemplary guidance, and constant encouragement.

I would like to extend my gratitude to **Dr. Asima Siddiqa,** Senior Scientific Officer, National Centre for Physics (NCP), Islamabad, and **Dr. Sajid Iqbal,** Principal Scientist, Pakistan Institute of Nuclear Science and Technology (PINSTECH), Islamabad for their encouragement, professional guidance and support during my research.

I am very thankful to my parents, my siblings, and my friends especially Ahmed Atiullah, Sabih ud Din, Nudrat Ehsan, Sana Rubab, Safa Zahoor and Fariah for helping me ou with their experiences and moral support. I am thankful to you all for being cooperative, supportive, and always being there to help. I wish you all the best.

Subul Huda

LIST OF TABLES

LIST OF FIGURES

HIGHLIGHTS

- Ni (II), Co (II), Cu (II) and Cd (II) being primary inorganic pollutants are toxic for both humans and animals
- The present work investigates the adsorptive removal of Ni (II), Co (II), Cu (II) and Cu (II) using $MgFe_2O_4$/ AC
- $MgFe_2O_4$/ AC showed removal efficiency between 98-99% for Cu (II), Co (II), Cd (II) and Ni (II) at 25 ppm
- $MgFe_2O_4$/ AC exhibited a selective removal of Cu (II) up to 99% as compared to other selected metals
- $MgFe_2O_4$/ AC has the tendency to be regenerated and reused

GRAPHICAL ABSTRACT

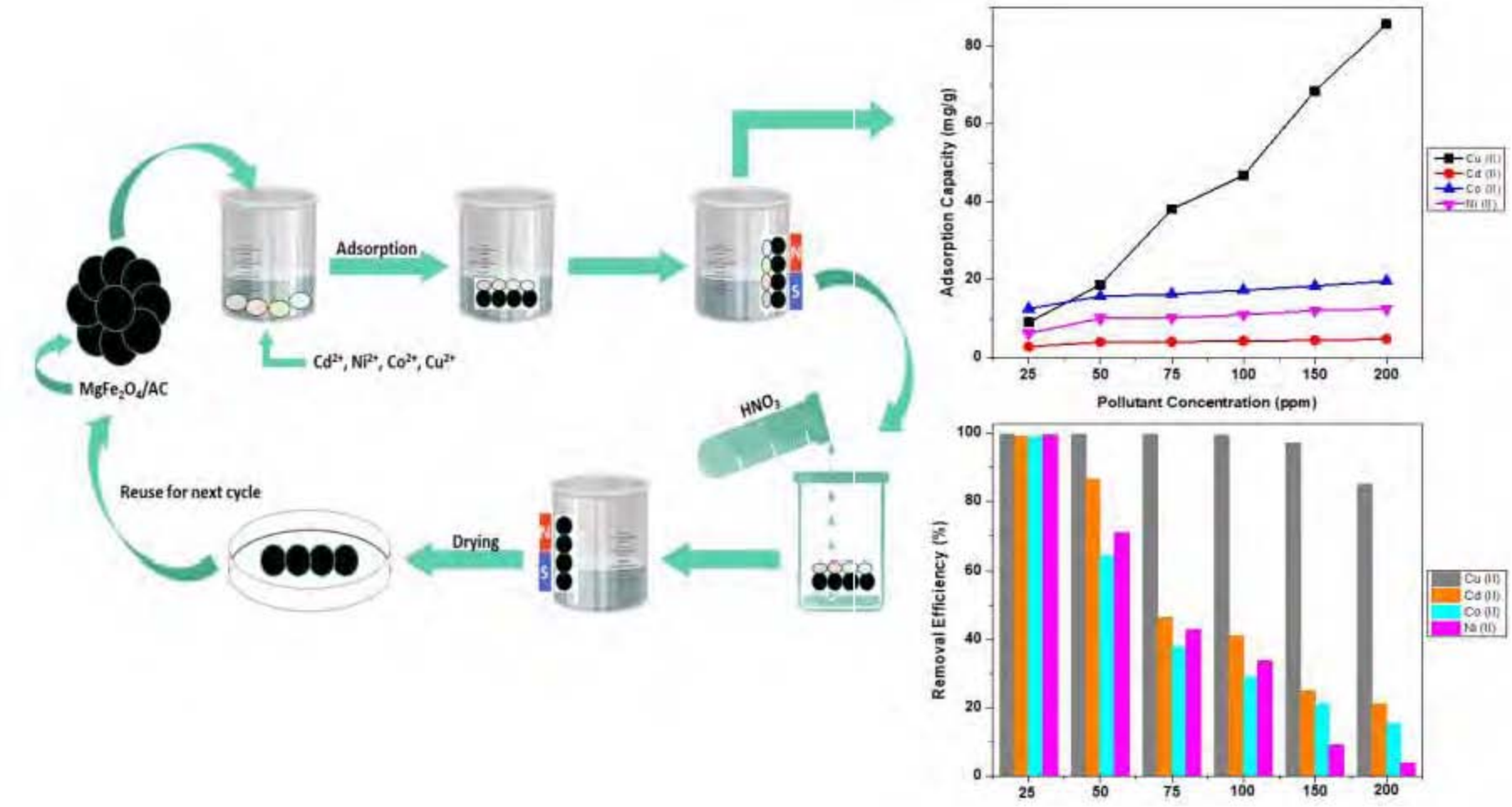

ABSTRACT

$MgFe_2O_4$/ AC has been synthesized using coprecipitation method. As prepared nanoadsorbent was characterized with various techniques such as Fourier Transform Infrared Spectroscopy (FTIR), Scanning Electron Microscopy (SEM) and Energy Dispersive X-ray Spectroscopy (EDS). The synthesized $MgFe_2O_4$/ AC nanocomposite was tested as adsorbent for simultaneous heavy metal removal; Ni (II), Co (II), Cu (II) and Cd (II) usually present in water and wastewater. In comparison better removal efficiency of Cu (II) was observed as compared to Cd (II), Co (II) and Ni (II) in this study. The influence of adsorbent dose, contact time, metal ion concentration, and pH were also investigated. The synthesized $MgFe_2O_4$/ AC nanoadsorbent shows the maximum removal efficiency of 99% for copper ions. A separate experiment was performed for the simultaneous removal of Cd (II), Co (II) and Ni (II) in the absence of Cu (II) which showed that their removal efficiency significantly increased in the absence of copper ions and that copper is selectively removed by $MgFe_2O_4$/ AC under all conditions. Although reported earlier, $MgFe_2O_4$/ AC did not exhibit excellent reusability in this study due to workup loss in consecutive cycles. This work provides an example to further explore the role of $MgFe_2O_4$/ AC for the selective adsorptive removal of Cu (II) in wastewater and exploring spinel ferrite nanocomposites for simultaneous removal of heavy metals.

1. INTRODUCTION

1.1. Background

Industrialization and agricultural practices have covered the significant gap between supply and demand created because of overpopulation and urbanization. Despite many astounding scientific developments, the expanding industrial revolution has also exacerbated problems with water contamination, putting all life on Earth in jeopardy. Numerous anthropogenic activities like mineral processing, metallurgical operations, mining and the production of pesticides, fertilizers, and several other chemicals, inorganic, organic, biological, and polymeric pollutants are continuously dumped into water resources, negatively damaging both terrestrial and aquatic flora and fauna[1]. In addition, the advancement in these practices has led to increased water use and water contamination. Throughout the past few years, the situation has worsened and led to global water crisis and water quality issues[2]. Due to such risk, it has become inevitable to enhance water treatment technologies, that must specifically be based on environmentally friendly systems of water management and can alleviate the water shortage[3]. Urbanization has also caused an increase in the production of municipal wastewater[4]. The most crucial phase is wastewater recovery and recycling[5]. The population's increasing usage of natural water resources affects composition, complexity, property, variability, and toxicity of the various kinds of wastewater pollutants[6]. The complexity of the wastewater then becomes a main obstacle in effluent treatment, increasing the danger of water contamination. In accordance with WHO recommendations, appropriate water treatment technologies can provide access to pure and clean water[2]. Therefore, the need for effective water treatment is currently existent, and several water treatment procedures can be used to achieve this[7].

The three main categories of water and wastewater contaminants are pathogens, harmful organic and inorganic pollutants. To begin with inorganic contaminants, they typically account for 30% of wastewater pollutants and include polyatomic chemicals and heavy metals[1]. These pollutants are frequently reported through a variety of environmental and water supply treatment processes in sectors such petroleum, textile, refining, pulp and steel,

and agri-food[8,9]. The highly bioavailable heavy metals and polyatomic substances have been linked to a variety of human ailments, including skeletal deformities and cardiovascular disease[10].

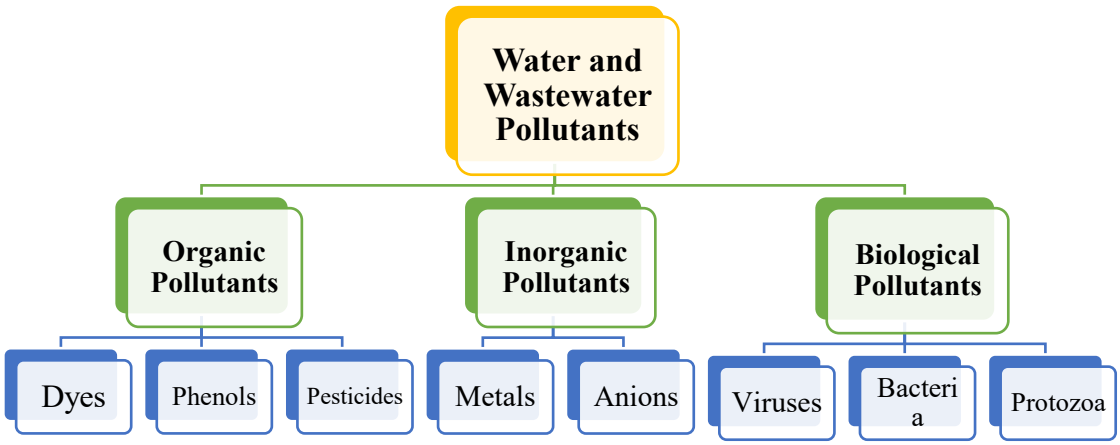

Anthropogenic factors may be responsible for the primary point sources of heavy metal contamination. Aqueous waste streams from various industrial sources, including electroplating operations, mining operations, power plants, and others, contain heavy metals[1]. These industries occasionally leave their waste streams behind, which causes the nearby soils, surface water, and ground water to become contaminated. Inorganic chemical pollution of the aquatic environment is thought to pose a serious hazard to aquatic creatures, especially fish. Large amounts of inorganic anions and heavy metals are added to the water bodies and sediment by agricultural drainage water that contains pesticides, fertilizers, runoff from industrial processes, and sewage effluents[11]. Industrial processes, petroleum contamination, and sewage disposal are the primary human-caused sources of metals[1]. Nickel, cobalt, copper, and cadmium are some of these heavy metals that are released into the water reserves and pose threats to humans, animals, and plants. The sources and toxicity of these metals are mentioned below.

1.2. Sources and Toxicity of Ni, Co, Cu, and Cd

1.2.1. Nickel

Nickel is widely present throughout the natural world and is the 24th most abundant element in the earth's crust, nickel is widely spread throughout the natural world. The main industrial application and hence a source of nickel include electroplating, alloy fabrication and production, cadmium-nickel battery and electronic component production, and catalyst creation for methanation and hydrogenation of lipids. In addition to symptoms including headache, giddiness, coughing, and shortness of breath, acute toxicity of nickel causes GIT symptoms such vomiting, nausea, abdominal pain, and diarrhea. Human pulmonary and digestive systems are also impacted by nickel salts. Exposure to more than 1 ug/L soluble nickel compounds also increases the risk of respiratory tract cancer[11]. Nickel also has an impact on the immunological, liver, kidney, and blood systems[12]. There is some evidence linking nickel exposure to human lung and nasal sinus malignancies. Metallic nickel is teratogenic and carcinogenic to mammals[11] causes lung, nasal and bone cancer at higher concentrations. The most common side effect of exposure to nickel present in jewelry and coins, is dermatitis (Ni itch). Tightness and pain in the chest pain, shortness of breath, a dry cough, fast breathing, cyanosis, and significant weakness are symptoms of acute Ni (II) poisoning[13].

1.2.2. Cobalt

Smaltite ($CoAs_2$) and cobaltite (CoAsS) are the two main minerals that contain cobalt, which makes up only 4% of the earth's crust. Common oxidation states of cobalt are (II) and (III)[11]. Cobalt is one of the many types of heavy metals that are utilized extensively throughout a variety of industries, including mining, galvanizing, metallurgy, petrochemistry, electroplating, paints, and pigments[14]. Additionally, cobalt and its salts are utilized in the production of vitamin B12, batteries, semiconductors, beer foam stabilizers, grinding wheels, nuclear power plants, and catalysts[14]. Because it is a component of vitamin B12, cobalt is necessary for humans. However, if it is present in larger amounts, it can harm the thyroid and liver as well as induce asthma, diarrhea, paralysis, pneumonia,

irritations in lungs, loss in weight, vomiting, and nausea. Additionally, excessive cobalt consumption has been linked to both carcinogenic and mutagenic outcomes[14].

1.2.3. Copper

A very prevalent metal called copper occurs naturally in the environment and spreads via natural processes. Copper can form in two different forms: Cu(I) and Cu (II). Copper has been one of the most frequently utilized metals as industries have developed. Printed circuit boards, metal finishing industries, tanneries, chemical manufacturing, and mine drainage are the main industrial waste sources for copper[11]. Over the past few decades, copper output has increased, which has led to an increase in the amount of copper in the environment. An enzyme involved in hemopoiesis called dihydrophil hydratase can be inhibited by an excess of copper in the body. Furthermore, Wilson's disease is an inherited disease that results in the body retaining copper because the liver does not eliminate it into the bile[11]. Damage to the liver and brain may result from this illness if it is not treated. It has also been discovered that excessive copper in water harms marine life. Higher copper concentrations have been found to harm fish and other animals, causing harm to their gills, liver, kidneys, and central nervous systems[11].

1.2.4. Cadmium

Cadmium occurs naturally in combination with zinc in Earth's crust. Rock weathering causes cadmium to be released to the water bodies; while some cadmium is added into the air by forest fires and volcanoes, the remaining amount of cadmium is released due to anthropogenic activities like manufacturing[11]. In addition to that batteries, paint pigments, fertilizers, mining, and alloy production are some of the main cadmium sources released into waste and water streams[15]. Ni-Cd batteries use over three-fourths of the available cadmium, with most of the remaining $1/4^{th}$ going toward pigments, coatings, electroplating, and stabilizing agents for plastics[16]. Cadmium is generally taken up by our bodies through diet, and tends to build up in the body, with 33% of it ending up in the kidney and 14% in the liver. Cadmium can affect the kidneys, the lungs, the bones, and even cause cancer and hypertension in people[15]. Itai-Itai, a sickness brought on by cadmium exposure, was

originally one of Japan's four major pollution disorders[11]. Other deteriorating effects to health that can be brought on by this poisonous metal cation include immune system and nervous system problems, nephrotoxicity, stomach pain, reproductive problems, psychiatric issues, and failures. Additionally, research on animals have shown that prolonged inhalation exposure to cadmium increases the risk of developing lung cancer, and EPA, U.S.A has designated cadmium as a potential human carcinogen[11].

Table 1 Sources and toxicity of Ni (II), Co (II), Cu (II) and Cd (II)

Sr. No.	Heavy Metal	Source	Toxicity	Permissible Limit	Ref.
1	Ni (II)	Alloys and manufacture of batteries, nickel plating industries	Carcinogen, loss of hair and skin toxicity in hypersensitive humans	0.02 ppb	[17]
2	Co (II)	Metallurgy, mining, electroplating, tanning, paint industries and nuclear power plants.	Skeletal deformities, diarrhea, hypotension pulmonary issues and paralysis	Not specified by WHO	[17]
3	Cu (II)	Battery manufacturing, and corrosion of household plumbing.	Headache, depression, and learning problems.	1.3 ppm	[18]
4	Cd (II)	Electroplating, metal smelting, paints, batteries, fertilizers, and alloying.	Renal dysfunction, pulmonary problems, bone tumors, high blood pressure, ItaiItai disease, and bone deformities in fetus	10 ppb	[15]

1.3. Conventional Methods for the Treatment of Heavy Metals

The treatment of wastewater and drinking water is one of the key criteria for growth, expansion of the economy, and maintenance of health in any part of the world. Therefore, it is essential to design and apply innovative technologies for water treatment that have improved energy efficiency. Waterborne illnesses continue to be a leading cause of death worldwide, particularly in developing nations where access to clean water is sometimes scarce. The contaminants must be removed from water to protect human health and the environment. Conventional treatment methods like reduction, precipitation, adsorption, oxidation, and ion exchange are frequently utilized for this purpose.

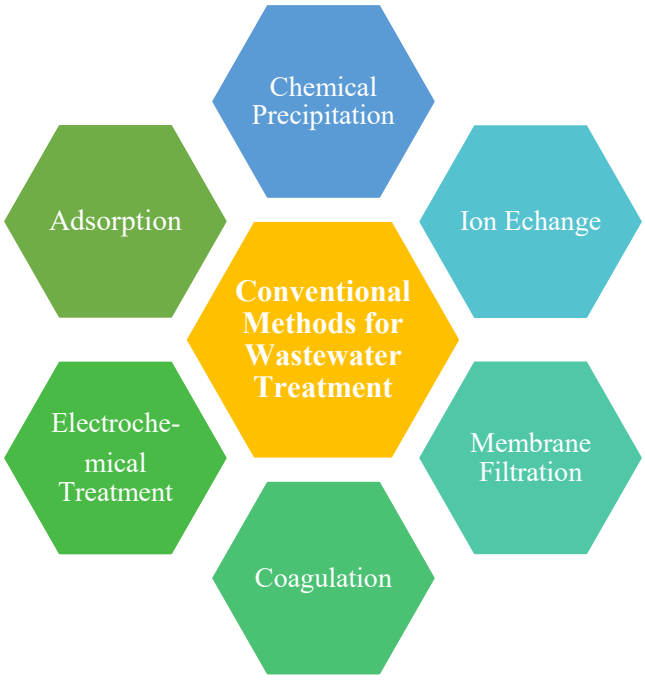

Figure 1 Conventional methods for the treatment of wastewater

1.3.1. Chemical Precipitation

Chemical precipitation is efficient and, so far, the most popular method in industry[19], because to its low operating costs and ease of usage. Heavy metal cations and chemicals

react during precipitation processes to form insoluble precipitates. Filtration or sedimentation can be applied to separate the precipitates from the water. After being decanted, the purified water is then properly recycled or released. Sulfide or hydroxide precipitation are two examples of preferred chemical precipitation processes[11].

1.3.2. Ion Exchange

The removal of metal ions from the solution through ion exchange involves the exchange of anions or cations between the effluent and the exchange medium occurs to remove the metal ions from the liquid phase through ion exchange[20]. In addition to natural or artificial organic materials, inorganic polymeric materials are employed to create mediums for ion exchange. Although this method of wastewater treatment is effective, it is not very popular because of its huge cost. Yet another drawback of this approach is that these ion exchange resins can absorb and store many hazardous chemicals that should necessarily be discarded through the ion exchange process[11].

1.3.3. Coagulation

The removal of toxic metals from wastewater can also be done by coagulation, followed by sedimentation and filtration[21–23]. Colloids are destabilized by coagulation by removing the forces holding them apart. Typically, coagulation cannot entirely remove the heavy metals from the effluent[24]. Other forms of treatment must therefore come after coagulation such as precipitation and flocculation.

1.3.4. Membrane Filtration

Because of its ability to remove all suspended solids, organic components and as well as inorganic pollutants such as heavy metals, membrane filtration has drawn great attention as a treatment method for heavy metals. Different forms of membrane filtration, including reverse osmosis, ultrafiltration and nanofiltration, can be used to treat toxic metal cations depending on their particle size which can be retained. Between ultrafiltration (UF) and reverse osmosis, nanofiltration (NF) is regarded as an intermediary process (RO). The removal of heavy metal ions from wastewater, including nickel[25], chromium[26], copper[27,28],

and arsenic[29,30], is possible with NF. A semi-permeable membrane is used in the reverse osmosis (RO) process, which allows the fluid being cleaned to pass through the membrane under pressure while rejecting the pollutants. Ni (II) and Cu (II) ions were successfully eliminated by reverse osmosis, with rejection efficiencies of up to 99.5 percent for the two ions[11].

1.3.5. Electrochemical Treatment

Electrochemical techniques can recover metals in the elemental state of metals by plating metal cations on a cathode surface. Electrochemical wastewater technologies have not been widely used because they require a significant capital investment and a costly electrical supply. In heavy metals removal from industrial effluent, EF offers a wide range of uses. Belkacem et al. looked at the use of aluminum electrodes and the EF technique for wastewater clearing[31]. Upon separation of a few metal ions, including those of Fe, Ni, Cu, Zn, Pb and Cd, the use of the optimum parameters was investigated. Their research showed that a 99 percent metal removal rate was possible. To improve the treatment of heavy metals, present in contaminated wastewater, electrochemical precipitation (EP) has been used and applies electrical potential to alter the traditional chemical precipitation process.

Figure 2 Basic principle of different methods for heavy metal removal [32]

1.4 Limitations of Conventional Methods

Although these techniques can be applied for the removal of toxic heavy metals from water and wastewater, the optimal technique should be able to meet the criteria of highest pollutant concentration set by the state as well as being adequate, relevant, and applicable to the actual conditions. Heavy metals can be isolated from other inorganic contaminants in wastewater using traditional treatment techniques. However, employing these techniques has several disadvantages, including high energy requirements, partial metal ion elimination, the production of toxic waste discharge, and high cost because of the chemicals utilized. Additionally, such procedures have less efficiency, call for delicate working settings, produce more sludge, and require expensive disposal. In wastewater sources having heavy metals and other organic pollutants, the presence of a single metal species frequently prevents the eradication of the others. In most cases, metal-containing wastewater is treated using conventional methods; yet these methods are not effective when heavy metals are present in lesser concentrations and produce more sludge, whose removal is difficult.

1.5 Adsorption

It is a surface process and is a popular method for the treatment of all kinds of pollutants. The interaction between a solid adsorbent having a highly porous surface structure and an adsorbable solute causes the adsorption process to occur. The solute molecules are concentrated on the surface of the adsorbent due to the attractive interactions between the solute and the adsorbent. The concentration of the adsorbate on the surface of adsorbent rises as an outcome of the adsorption process[33]. Adsorption is regarded as a particularly suitable technology for the purification of wastewater among all other methods mentioned above because of its high efficacy, affordability, diversity, and ease of control[34,35]. The adsorbents are mostly inexpensive and do not require any prior processing before use. Thus, ecologists throughout the world frequently use the adsorption technique to remove harmful and poisonous inorganic and organic contaminants from water and consider it to be one of the finest options for water treatment.

1.5.1 Types of Adsorption

Adsorption methods are divided based on the kind of the surface attachment which can be physical, chemical or exchange adsorption[33]

1. Physisorption or physical adsorption happens due to Van der Waals forces and is separated most easily because of the weak nature of the forces. It does not include transfer or sharing of electrons, and it is essentially reversible.
2. Chemisorption or chemical adsorption happens through formation of chemical bonds between adsorbate and adsorbent. Chemisorption occurs only as a monolayer. Furthermore, materials that are chemisorbed on a solid surface are difficult to remove. It is principally irreversible. Under favorable conditions, both processes can occur simultaneously or alternately.
3. Ion Exchange or exchange adsorption is caused by the electrostatic attraction between adsorbate and the adsorbent surface.

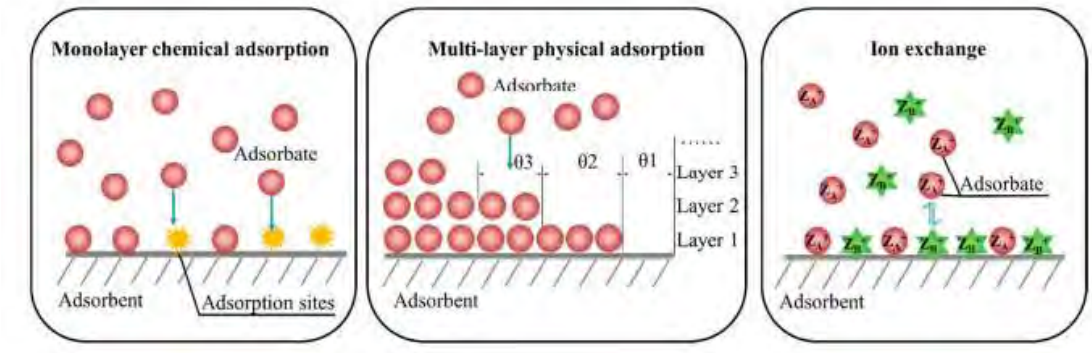

Figure 3 Different possible mechanism of adsorption [36]

1.5.2 Factors Affecting Adsorption Process

Heavy metal ion adsorption over diverse surfaces is influenced by several variables, including the initial concentration of ions, time of contact, dose of adsorbent, and reaction media pH[37]. As a result, the following sections will describe how the aforementioned factors affect the removal of heavy metals from water and wastewater.

1.5.2.1. Effect of Initial Ion Concentration

In general, it is understood that raising concentration of the pollutants increases the adsorption rate up to a specific point, after which the adsorption declines because of optimum concentration of metal ions which must be present in the medium for the particular adsorbent. Lesser concentrations of metals make it possible for the scavenging effectiveness to drop, but greater concentrations of metallic ions make it possible for the removal efficiency to grow. However, above a specific initial concentration, ions with the same number of accessible sites for adsorption are present, that reduces their elimination and hence the adsorption capacity[37].

1.5.2.2. Effect of Contact Time

The contact time between the adsorbent and the heavy metal ions is a key factor in the cost-effective treatment of hazardous metals from wastewater. The longer the period of contact between adsorbent and the pollutants, the more time there is for interactions between metals' active chelation sites and the pollutants to take place. The removal efficiency often starts off fast and then gradually improves during the adsorption process. This happens because initially available empty active sites during adsorption are eventually filled with chelated metals over time. As soon as the equilibrium between desorption and adsorption is reached, the adsorption ceases to depend on the contact time[37].

1.5.2.3. Effect of Adsorbent Dosage

In order to remove pollutants through adsorption, the dosage of the adsorbent is crucial. The existing active sites to chelate hazardous metals increased as the adsorbent dosage was increased, considerably enhancing the adsorption capacity. So, the dosage of nanoparticles effectively increases the sorption capacity. However, a further addition in the amount of adsorbent reduces the surface area as well as the active site due to agglomeration and hence negatively impacting the adsorption efficiency[37]. Various research has examined the impact of adsorbent dose on the heavy metals' removal from an aqueous solution. The Fe3O4@C nanoadsorbent was applied to discharge lead ions from water. When the dosage was increased to 2 from 0.5 g/L, the efficiency improved from 41% to 92%. This

improvement was caused by an augmentation in the number of active sites and the simple contact of Pb ions with these active sites. However, due to agglomeration of adsorbent, which limits the active sites left to form complex with Pb ions, the increase in adsorbent dosage resulted in a reduction in removal efficiency from 41% to 22%[38].

1.5.2.4. Effect of pH

The pH of the reaction medium has a consequential impact on both the reaction and the adsorption capacity. Thus, it is necessary to ascertain how pH affects the scavenging of metal ions. According to various research, intermediate pH values are preferred to lower pH values for the adsorption of heavy metals. Although the number of protonated active sites increases at low pH and causes a strong repulsion to positively charged hazardous contaminants, this significantly lowers the nanoadsorbent's capacity for adsorption[39]. When the pH level is extremely high, a lot of complexes between metal cations and OH^{-1} species develop, blocking a significant portion of active sites on the adsorbent and lowering the adsorption capacity[37].

1.6 Application of Nanotechnology in Treatment of Water and Wastewater via Adsorption

To eliminate organic and inorganic impurities from wastewater and water, sorbents are frequently employed in the tertiary treatment and purification process. Efficiency of common sorbents, like activated carbon and ion-exchange resins, used in adsorption processes. suffer from low selectivity and specificity, low accessible surface area or active sites, and poor adsorption kinetics[11]. Due to the greater surface area of nanoparticles, their substantial selectivity and specificity, as well as their adjustable surface chemistry and pore size on a huge basis, the use of nanomaterials (also known as nanosorbents) may have advantages over conventional materials (also known as sorbents) to overcome difficulties. Additionally, some nanoparticles can be particularly effective adsorbents due to their peculiar electric and structural characteristics[11]. There are very few commercialized nanosorbents, mostly from the United States and Asia, but a lot of research is being done on a variety of specific water pollutants.

1.7 Development of Nanoadsorbents for Wastewater Treatment

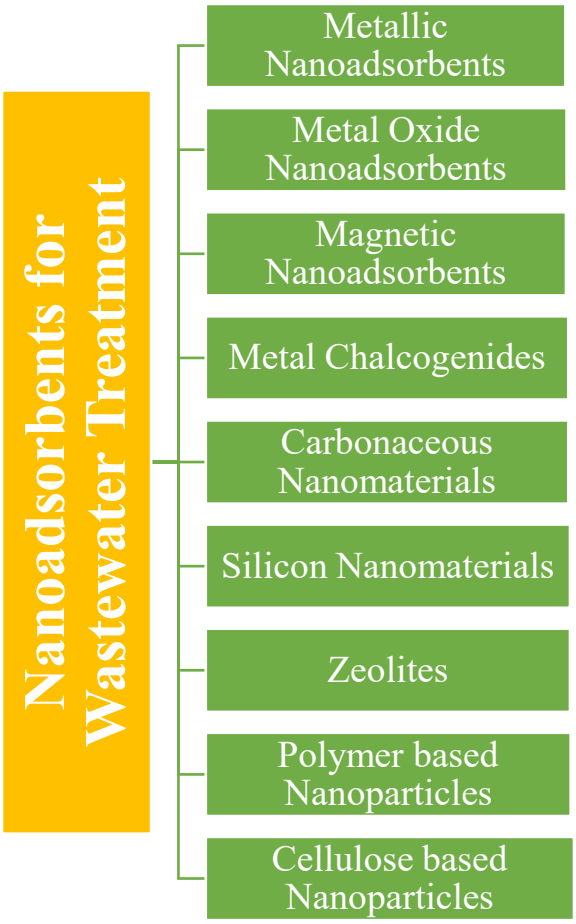

Based on chemical composition and functionalization, which alter the behavior of their surface adsorption sites, nanoadsorbents are divided into distinct categories. These categories are given as below:

a) Metallic nanoadsorbents: Several nanostructured and functionalized Au nanoparticles, Ag nanoparticles, Cu nanoparticles, Ni nanoparticles, Pt nanoparticles, and Pd nanoparticles[40].
b) Metal oxide nanoadsorbents: Multiple nanostructured and functionalized zinc oxide, magnesium oxide, calcium oxide, titanium oxide, copper oxide, tin oxide, nickel oxide and manganese oxide etc[40].
c) Magnetic nanoadsorbents and nanocomposites: Several functionalized and nanostructured Fe_2O_3, Fe_3O_4, Co_3O_4, NiO_2, ferrites such as $CoFe_2O_4$, $NiFe_2O_4$,

$MnFe_2O_4$, $ZnFe_2O_4$, and $CuFe_2O_4$; manganese compounds; core–shell structure etc[40].

d) Zeolites[37]
e) Carbon nanomaterials (CNMs): Carbon nanotubes (CNTs), carbon nanoparticles (CNPs), graphene and their functionalized materials[40].
f) Cellulose based nanoparticles[37]
g) Metal chalcogenide nanoadsorbents: Several nanostructured and functionalized MoS_2, MnSe, WS_2, MnS, $MoSe_2$, CuS, WSe_2, NiS, CoS, FeS, Fe_2S_3, etc[40].
h) Polymer based nanoparticles such as chitosan[37]
i) Silicon nanomaterials (SiNMs): silicon nanoparticles (SiNPs), silicon nanotubes (SiNTs), and silicon nanosheets (SiNSs)[40].

Examples of these nanoadsorbents that have been applied for removing heavy metals being analyzed in this study are presented in **table 2**.

Table 2 Various adsorbents for the removal of Ni (II), Co (II), Cu (II) and Cd (II)

Metal Ions	Adsorbent	Initial Metal Conc. (mg/L)	Adsorbent Dose (mg/L)	Ref.
Ni (II)	(PVA)/NaX nanozeolite	50	500	[41]
	SPH	100	2	[42]
	HDI-IC-PEHA	58.6, 63.8, 51.9	1000	[43]
	Alg-CS	70	3000	[44]
	(PVA)/zinc oxide (ZnO) nanofiber	50	1000	[45]
	DTZ-Al2O3 and MAB-Al2O3)	17.5-368.5	3330	[46]
	SNHS, NH2–SNHS, (NH2–SG)	140	15	[47]
Co (II)	Graphene oxide nanosheets	20	1000	[37]
	Al_2O_3 NPs in zeolite	50	-	[48]
	SPH	100	2	[42]
	HDI-IC-DETA	58.9, 112.4	1000	[43]
Cu (II)	SPH	100	2	[42]
	PAN nanofibers	100	1000	[49]
	HDI-IC-PEHA	58.6, 63.8, 51.9	1000	[43]
	Fe_3O_4	2	10	[50]
	NH_2 silica	-	1000	[51]
Cd (II)	Graphene oxide nanosheets	20	1000	[37]
	(PVA)/NaX Nanozeolite	50	500	[41]
	SPH	100	2	[42]
	HDI-IC-DETA	58.6, 63.8, 51.9	1000	[43]
	NTA – Silica gel	20		[52]

1.7.1 Magnetic Nanoadsorbents

Magnetic nanoparticles are the primary class of advanced nanomaterials that enable both enhanced harmful metal removal and simple magnetic separation. After separation, this class of nanomaterials brings exceptional recyclability, providing ecological advantages and a broad range of applications for remediation of environment. The characteristics of such nanomaterials dramatically alter as their size decreases. Since the difficult separation and limited surface area, non-magnetic nanoparticles are not much effective in treating water than magnetic nanomaterials. The magnetic nanoparticles, on the other hand, have a huge surface area, are chemically inert, are less hazardous, and are easily disseminated. These characteristics of magnetic nanoparticles make them reliable, affordable, and useful for the purification of water. Thus, employing these nanomaterials effectively allows for the removal of heavy metals[37]. Magnetic nanoparticles make separation simple and affordable using a strong magnetic field. Because of their magnetic features, magnetic adsorbent works as both an adsorbent for treating harmful metals from solutions and a magnetically energized source for attracting and holding paramagnetic nanoparticles that can also be removed[53]. The benefit of this separation technology is that a straightforward magnetic field can remove the dangerous chemicals and the magnetic particles from the treatment system. The undesirable elements can frequently be eliminated from the magnetic particles after separation in the external magnetic field, allowing for reuse of the magnetic particles. The magnetic adsorption process is more inexpensive and has the potential to replace the widely used filtration and centrifuge separation technologies because of easier operation and lower regenerative process costs[53].

According to research, magnetic nanoparticles are advantageous because of a large surface area, a large number of surface-active sites, and high magnetic properties, that result in enhanced adsorption efficiency, an increased rate of contaminant removal, and simple, quick separation of adsorbent from solution via the magnetic field. Additionally, after magnetic separation by an external magnetic field, it's feasible that the dangerous elements can be taken out of the magnetic particles, allowing them to be recycled[53].

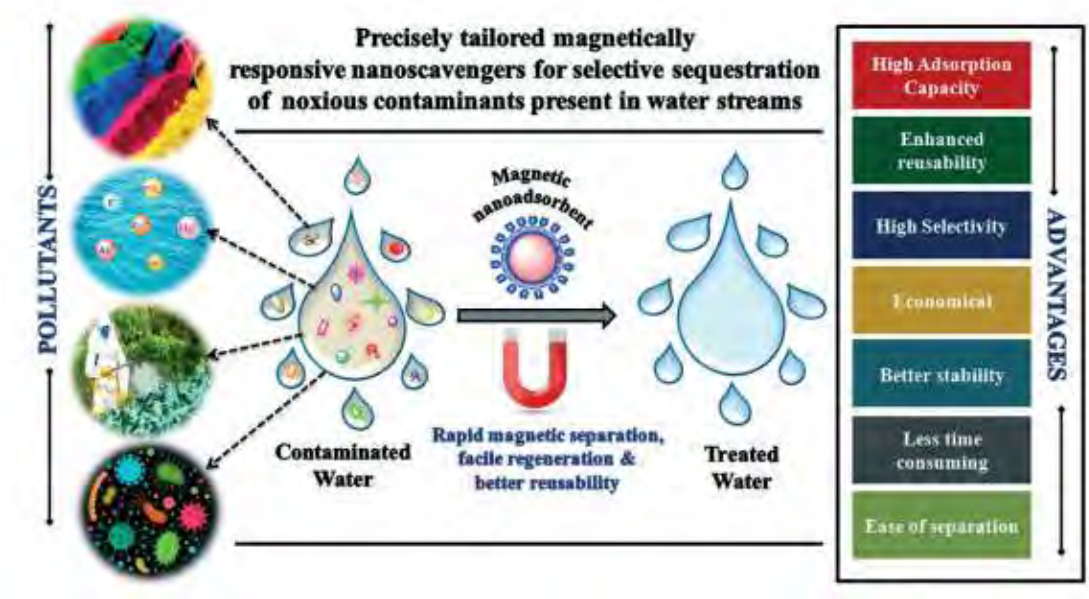

Figure 4 Magnetic nanoadsorbents for the treatment of different pollutants [32]

Due to their tendency towards oxidation, magnetic nanoparticles show easy aggregation in water, and hence have few practical applications. Along with the development of their synthesis, it is crucial to avoid the precipitation or aggregation of the magnetic nanoparticles. To solve these issues, bare magnetic nanoparticles were functionalized. Magnetic nanoparticles' surface functionalization improved their selectivity, stability, and adsorption ability[37]. The presence of variable functional groups over magnetic surfaces brings about different types of interactions between metals and surfaces, such as Van der Waals, chemical binding, ligand combination, electrostatic and complex formation. Furthermore, by functionalizing charged moieties, electrostatic interactions on metal surface can be improved. Thus, increased electrostatic attraction was primarily responsible for the selectivity of surfaces toward certain metals[37]. Additionally, functionalization improved the homogeneity and high surface area of magnetic nanoparticles. The characteristics of the magnetic surfaces were changed to enable selective chelation of hazardous metals. The size and surface area of magnetic nanoparticles, which are strongly influenced by surface modification, determine their selectivity and enhancement of adsorption toward harmful contaminants. Magnetic nanoparticle surfaces were altered

through numerous experiments using a variety of modifiers, including carbonaceous, biomolecular, inorganic, organic, and polymer components, among others[37].

1.7.2. Magnetic Nanocomposites

Nanocomposites are multiphasic materials and are defined as matrix materials reinforced with at least one dimension (100 nm)[54]. In order to create unique functional materials that meet the requirements of a certain application, they combine the properties of nanosized filler and matrix material. Numerous host materials, including silica, liquid media, and organic polymers, are frequently used in nanohybrids[54]. Particularly, host materials that exhibit desirable characteristics and respond to external stimuli are of interest. Due to a variety of benefits, such as comparatively large penetration depth, magnetic field as an external stimulus has received a lot of interest in this regard[55]. The matrix host contains magnetic nanoparticles that can be disseminated in various materials and that, when exposed to static or substitute magnetic fields, exhibit unusual properties that cause them to react to the external magnetic field. Magneto-mechanical forces are produced by the interaction of magnetic field gradient and particle magnetic moments, and they can be used to detect changes in the shape or motion of the host material. Several uses, including medication delivery and magnetic separation, are possible for this[56].

Table 3 shows several magnetic nanoadsorbents that have been synthesized for the treatment of heavy metals including Ni (II), Co (II), Cu (II) and Cd (II).

Table 3 Magnetic nanoadsorbents for the treatment of Ni (II), Co (II), Cu (II) and Cd (II)

Heavy Metal	Magnetic Nanoadsorbent	Reference
Ni (II)	Fe3O4	57
	Fe3O4@ Carboxymethyl-β-cyclodextrin	58
	Fe3O4@SiO 2@SiO2-SH	59
	Fe3O4@Gum kondagogu	60
Co (II)	Succinic acid- Fe3O4	61
	Magnetite/ Graphene oxide	62
	Chitosan - Fe3O4	63
	MgFe2O4	64
Cu (II)	γ-Fe2O3 nanotubes	65
	Fe3O4	57
	Fe3O4@ Chitosan	57
	Fe3O4@ Humic acid	57
Cd (II)	Fe3O4	57
	Fe3O4-α- Fe2O3 mixture	66
	Fe3O4@ Chitosan	67
	Fe3O4@ Carboxymethyl-β-cyclodextrin	58
	ɣ-Fe2O3@ Polyrhodanine	68

1.7.3 Magnetic Carbon Nanocomposites

In addition to being polymer nanocomposites, magnetic carbon nanocomposites are also known as such because they use carbon as their hosting matrix[69] (Behrens 2011). Due to its many properties, including chemical stability, conductivity, mechanical strength, and high anisotropy, carbon has been the most extensively explored material. In previous years, a variety of carbon structures have been synthesized, including expanded graphite and graphene, carbon nanotubes (CNTs), carbon nanofibers, buckminsterfullerene (C60) and as well as activated carbon (AC). In many cases, amazing magnetic properties are seen

when these carbon compounds are combined with magnetic nanostructures[54]. The very effective materials known as magnetic carbon nanocomposites can bring about beneficial changes in a variety of processes. Additionally, the porous morphology of magnetic carbon nanocomposites makes it easier to use them in fields like environmental remediation, catalysis, and as an electrode[70,71]. The numerous fabricated magnetic carbon nanocomposites over the past few years includes magnetic hydrochar nanocomposite, magnetic carbon nanospindles, carbon nanotube/magnetite coaxial nanocables, magnetic biochar/polypyrrole (PP) nanocomposite, carbon-coated magnetic nanoparticles, magnetic multi-walled carbon nanotube heterojunction, iron oxide/graphene nanocomposite, iron encapsulated carbon sphere, zinc coated iron oxide-carbon hollow sphere and spinel ferrite activated carbon or spinel ferrite graphene nanocomposites[54,72,73].

1.8 Spinel Ferrite Nanoparticles and Spinel Ferrite Nanocomposites

Due to their unique superparamagnetic (SPM) characteristics, surface area to volume ratio, and high adsorption capabilities, magnetic nanoparticles (MNPs) have received a lot of interest lately. Ferrites are one of the most significant MNPs and are comprised of transition metal oxides with spinel structures. Ferrites are categorized as garnet ($M_3Fe_5O_{12}$, where M = rare earth cations), orthoferrite ($MFeO_3$, where M = rare earth cations), hexaferrite ($SrFe_{12}O_{19}$ and $BaFe_{12}O_{19}$), and spinel (MFe_2O_4, where M = Mn, Fe, Co, Ni, Co, Zn, and so forth) based on their magnetic characteristics and crystal structures[74–76]. Spinel ferrite nanoparticles have received particular focus among these. This is mostly because of their superior magnetic capabilities, straightforward chemical composition, and broad range of applications in industries like wastewater treatment, biomedicine, catalysis, and electronic devices[77].

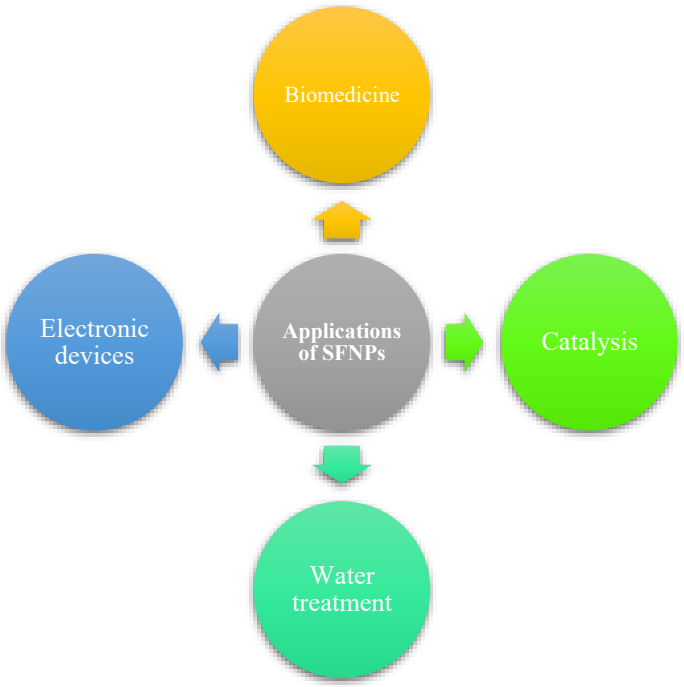

Figure 5 Applications of spinel ferrite nanoparticles

Spinel ferrites are homogenous substances having the chemical formula AB_2O_4, where A and B are metal cations located at two different crystallographic sites, tetrahedral (A sites) and octahedral (B sites), and where Fe (III) is one of their principal constituents. Both the cations are tetrahedrally and octahedrally coordinated to oxygen atoms, respectively. Three alternative spinel ferrite structures, namely normal, inverse, and mixed, are known for the formula MFe_2O_4 depending on the position of M (II) and Fe (III) site preference[77].

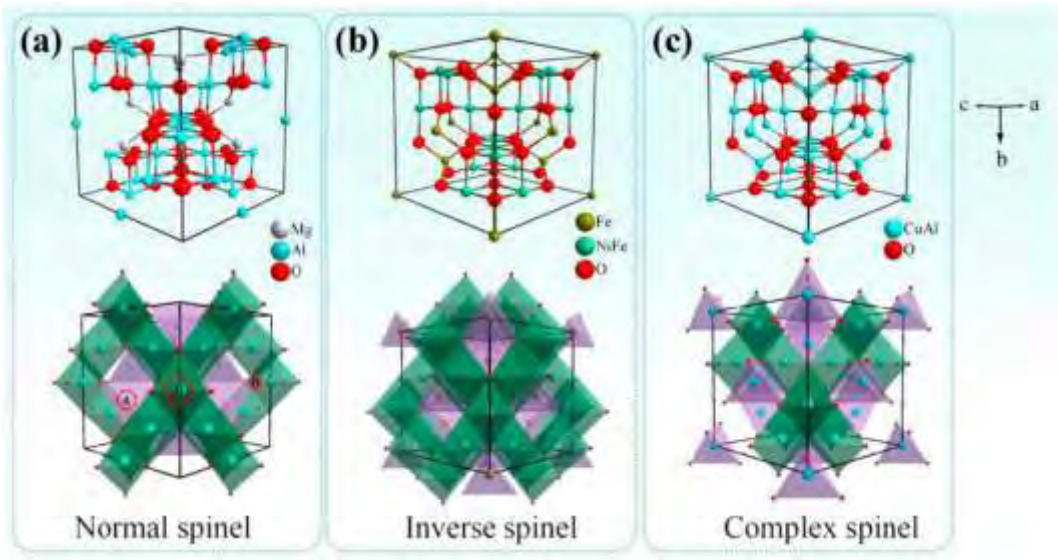

Figure 6 Crystal structures of different kinds of spinel ferrites

SFNPs have been utilized in industries for wastewater treatment to eradicate dyes[78,79], phenols[80,81], and toxic trace metals[82–86]. The possibility of reusing them several times and their ease of their recovery from the reaction mixture by external magnetic field are other additional benefits of SFNPs[87–89].

Industries have used SFNPs to remove dyes[78,79], phenols[80,81] and harmful trace metals[82–86] from wastewater. Another benefit of SFNPs is the simplicity with which they may be recovered from the reaction mixture using a magnet and the potential for multiple re-uses[87–89]. Other treatment options could be used to remove pollutants from water, but there are several issues that prevent their use, such as inadequate pollution removal, difficulty recovering adsorbent, cost-ineffectiveness, and in some cases, voluminous waste sludge that requires proper design and a lot of space to be disposed of[77]. Current adsorbents for wastewater treatment are ineffective because of the abovementioned reasons. Therefore, there is a need for a low-cost, efficient, easily recovered, and reusable adsorbent.

The best materials to use to solve issues with water quality and purification are SFNPs/SFNCs[77]. This is mostly because of their exceptional physical and chemical characteristics, which provide them with the ability to simultaneously remove a variety of contaminants and make them simple to recover and reuse. The advantages of SFNPs and

their equivalent SFNCs as compared to their bulk counterparts include higher adsorption capacity, cost-effectiveness, and contamination removal efficiency[79]. The ease of regeneration and the ability to reuse recovered and regenerated adsorbents for various cycles without losing their adsorption capacity also ensure SFNPs/SFNCs as one of the finest options, and they have recently become widely employed in water and wastewater treatment.

The use of an adsorbent in the treatment of wastewater and water is regarded as one of the most cost-effective alternate methods since the removal of undesired species through adsorption requires only simple working, is affordable, and does not produce secondary pollutants while the water or wastewater is being treated[90,91]. Because of their large surface area and increased active sites for interacting with pollutants, SFNPs are now favored for wastewater treatment[92]. In addition, SFNPs exhibit SPM behavior due to their nanoparticle size, which makes it possible for them to be removed from solutions by using an external magnet with ease.

The general formula of metal ferrite nanocomposite is $M(Fe_xO_y)$, where M is the metal atom. Many metal ferrites have been produced, including $ZnFe_2O_4$, $CuFe_2O_4$, and $Mn_{0.67}Zn_{0.33}Fe_2O_4$ for the removal of heavy metals[93,94]. With a strong adsorption capacity, $ZnFe_2O_4$ removed Pb^{2+} ions whereas $CuFe_2O_4$ removed Mo^{2+} ions from aqueous samples. Arsenic pentavalent ions, lead, and cadmium divalent ions were all successfully removed by $Mn_{0.67}Zn_{0.33}Fe_2O_4$. Another study produced nanoparticles using the co-precipitation approach to create cobalt and manganese spinel ferrites ($CoFe_2O_4$ and $MnFe_2O_4$) with a size range of 20-80 nm. With an adsorption capacity of 454.5 mg/g for $MnFe_2O_4$ and 384.6 mg/g for $CoFe_2O_4$, respectively, the produced nanoparticles removed divalent zinc ions[95]. Cobalt ferrite ($CoFe_2O_4$) magnetic nanocomposite was prepared by Vamvakidis et al. and subsequently modified by coating with octadecylamine. With a large adsorption capacity of 164.2 mg/g, the magnetic nanocomposite that was created absorbed copper divalent ions. The nanocomposite demonstrated relatively straightforward regeneration using an acidic treatment after being separated with a magnet[96].

1.8.1 Magnesium Ferrite/ Activated Carbon

Magnesium ferrite ($MgFe_2O_4$) is an N-type semiconducting material possessing magnetic character[97]. The Fe^{3+} ion is evenly distributed throughout the available tetrahedral and octahedral sites, making it an inverse spinel in bulk form. It is primarily employed in sensors, transformers, catalysis, ferrofluids, magnetic coil cores, and local hyperthermia treatment due to its high resistivity and minimal magnetic and electric loss[97]. At normal temperature, a crystallite exhibits superparamagnetic characteristics when its size falls below a predetermined threshold. The distribution of cations among the available lattice sites determines the chemical and physical characteristics of ferrites. As it crystallizes, magnesium ferrite forms mixed spinel. The tetrahedral (A-sites) and octahedral (B-sites) cation sites are denoted by parenthesis and square brackets, respectively, in the structural formula $(Mg_{1-x}Fe_x)$ $[Mg_xFe_{2x}]$ O_4[98]. The magnetic moment of $MgFe_2O_4$ is solely a result of the uncompensated spins of Fe ions dispersed in the tetrahedral and octahedral (A and B) sites because Mg^{2+} is a nonmagnetic ion.

When compared to other spinel ferrites, iron oxide-containing nanoparticles (NPs) such as magnesium ferrite nanoparticles ($MgFe_2O_4$ NPs) are more advantageous. They are said to be harmless and biocompatible and do not include hazardous heavy metal ions in the form of divalent cations[99]. They have a lot of surface-active sites and are stable, non-toxic, and insoluble in water[100]. $MgFe_2O_4$ NPs are more effective when used in the fabrication of nanocomposites due to their quick shorter intra-particle diffusion distance, kinetics, and capacity to recover magnetic material from solutions[101]. For adsorption of direct red 16 and methyl orange, magnetic nanocomposites comprising activated charcoal, multiwall carbon nanotubes, graphene, and graphene-oxide with spinel ferrites (M = Mn, Ni, Co, Zn) have been described[102–104]. In order to remove chromium, a nanocomposite of $MgFe_2O_4$ NPs with activated charcoal and bentonite was tested[105,106]. By acting as a reductant for Cr (VI) at lower pH, activated charcoal nanocomposite rendered to be more efficient in comparison to pure $MgFe_2O_4$ NPs.

One of the biggest disadvantages of transition metal ferrites (Mn^{2+}, Co^{2+}, Ni^{2+}, Cu^{2+}, etc.) is the leaching of toxic metals during the treatment process. This in result usually leads to

secondary pollution[99]. This nanocomposite is chosen for this study because, in contrast to ferrites made of transition metals, these materials are safe for use by humans and other living things[107]. The goal of the research is to examine how different variables affected the sorption characteristics of $MgFe_2O_4$ magnetic nanoparticles and $MgFe_2O_4$ activated carbon nanocomposite toward the ions Cd^{2+}, Co^{2+}, Ni^{2+}, and Cu^{2+} from one component aqueous solutions.

1.10. Problem Statement

The conventional wastewater treatment methods have certain limitations as discussed above. They require high energy, are expensive and do not treat lower concentrations of heavy metals. In addition, there is also incomplete removal of metal ions and high production of sludge. On the other hand, there are a few newly developed techniques that allow the simultaneous adsorptive removal of multiple heavy metals. Such issues create room for exploring new options. There is need for an environment friendly treatment method that can efficiently remove multiple heavy metals at one time, is inexpensive and can be reused.

1.11. Aims and Objectives

The research aim is to synthesize an efficient, environmentally friendly nanoadsorbent that can be employed for the simultaneous removal of heavy metals (Ni^{2+}, Co^{2+}, Cu^{2+} and Cd^{2+}). Objectives of this research are listed below:

1. To synthesize of magnesium ferrite/ activated carbon ($MgFe_2O_4$/ AC) nanocomposite
2. To test the efficiency of $MgFe_2O_4$/ AC for the adsorptive treatment of heavy metals (Ni^{2+}, Co^{2+}, Cu^{2+} and Cd^{2+}) in laboratory prepared samples
3. To study the effect of different parameters i.e., effect of concentration of metal ions, adsorbent dose, contact time and pH.
4. To evaluate the reaction kinetics and adsorption isotherm parameters of selected heavy metals adsorption.
5. To test the regeneration and reusability of synthesized nanoadsorbents.

2. METHODOLOGY

This chapter includes the descriptions of materials that are used in the synthesis of proposed system that is magnesium ferrite activated carbon nanocomposite. It also includes methods adapted for adsorption experiment and regeneration and reusability of the adsorbent. magnesium ferrite/ activated carbon ($MgFe_2O_4$/ AC)

2.1. Materials

Magnesium nitrate hexahydrate (Mg $(NO_3)_2.6H_2O$), iron sulfate ($FeSO_4$), sodium hydroxide pellets (NaOH) and activated carbon (AC) were required for the preparation of $MgFe_2O_4$ and $MgFe_2O_4$/ AC nanocomposite. Nickel chloride ($NiCl_2$), cobalt chloride ($CoCl_2$), copper sulfate ($CuSO_4$) and cadmium chloride ($CdCl_2$) are required for the preparation of heavy metal solution for adsorption experiment. Nitric acid (HNO_3) was used for the desorption of heavy metals from the adsorbent and its regeneration. Analytical grade chemicals were used and were not further purified before use.

2.2. Synthesis of Magnesium Ferrite/ Activated Carbon Nanocomposite

Magnetic $MgFe_2O_4$/AC nanocomposite was synthesized through coprecipitation method. 1M Mg $(NO_3)_2 \cdot 6H2O$ and 2M $FeSO_4$ were dissolved into 50 mL distilled water and magnetically stirred at room temperature. 4g of AC was added into the above solution at room temperature and allowed to stir for 2 hours. 2M NaOH solution was added dropwise until the pH in the reaction mixture reached 12. The reaction mixture was then magnetically stirred for another 8 hours at room temperature. The resultant precipitates were washed several times with distilled water to obtain a neutral pH value. The precipitates were dried at 100 °C for 8 hours and grinded into a fine powder using pestle and mortar. The powdered particles were laid into a 50 ml crucible and calcined at 600 °C for 2 hours to achieve a final product of blackish brown color. The identification of the synthesized compound was done via SEM/ EDS, and FTIR.

2.2.3. Characterization of $MgFe_2O_4$/AC

The following characterization was done for $MgFe_2O_4$/AC to study their material properties.

1. Scanning Electron Microscopy (SEM)
2. Energy Dispersive X-ray Spectroscopy (EDS)
3. Fourier Transform Infrared Spectroscopy (FTIR)

2.3. Preparation of Stock Solutions

1000 mg/l stock solutions of Ni, Co, Cu and Cd were prepared separately. For preparing the working solution, the required concentration of each heavy metal solution is taken in the same flask and diluted up to the mark. The dilution formula used to prepare the working solution from 1000 mg/l stock solution is

$$\boldsymbol{C_1V_1 = C_2V_2}$$

Where C_1 = 1000 mg/l

V_1 = required volume of the stock solution

C_2 = concentration of the working solution

V_2 = final volume of the working solution

2.4. Adsorption Study

Different parameters such as effect of initial metal concentration, adsorbent dose, contact time, and pH were studied to analyze the adsorption efficiency of $MgFe_2O_4$/AC. The samples were analyzed on inductively coupled plasma optical emission spectroscopy (ICP-OES). A final adsorption experiment was performed under optimum conditions determined from the effect of each parameter on adsorption. In the end the adsorbents were regenerated to evaluate their reusability.

2.4.1. Effect of Contact Time

A working solution having 100 mg/l of Ni (II), Co (II), Cu (II) and Cd (II) was prepared from the stock solution. A 30 mL aliquot of the working solution was taken in the 50 mL falcon tube. 70 mg of the adsorbent was added in each falcon tube separately. The prepared samples were thoroughly mixed and agitated at 150 rpm for 15, 30, 45, 60, 90, 120, 150 and 180 minutes. The adsorbent was magnetically separated, and the sample solutions were analyzed.

2.4.2. Effect of Adsorbent Dose

To evaluate the effect of adsorbent dose, 30, 50, 70, 100, 150, and 200 mg of $MgFe_2O_4$/AC were added in 30 mL of 100mg/L heavy metal solution. The samples were mixed thoroughly and agitated on the shaker at 150 rpm for two hours. After shaking, the adsorbent was allowed to settle down and then separated using an external magnet and the samples were analyzed.

2.4.3. Effect of Initial Metal Concentration

The effect of initial metal concentration on the adsorbent is studied by changing the concentration of the pollutant solution. 25, 50, 75, 100, 150 ppm of the heavy metal solution is taken with 70 mg/l of the adsorbent. The solutions are shaken for two hours after which the adsorbent is separated using an external magnet.

2.4.4. Effect of pH

To adjust the pH 1M HCl and 1M NaOH were used, and the pH values were maintained between 1-7 as metal ions precipitate and form metal hydroxides at higher pH. A 30 mL aliquot of the heavy metal solution was taken in which 70 mg of the adsorbent was added. The samples were shaken at 150 rpm for two hours. An external magnet was used to separate the adsorbent.

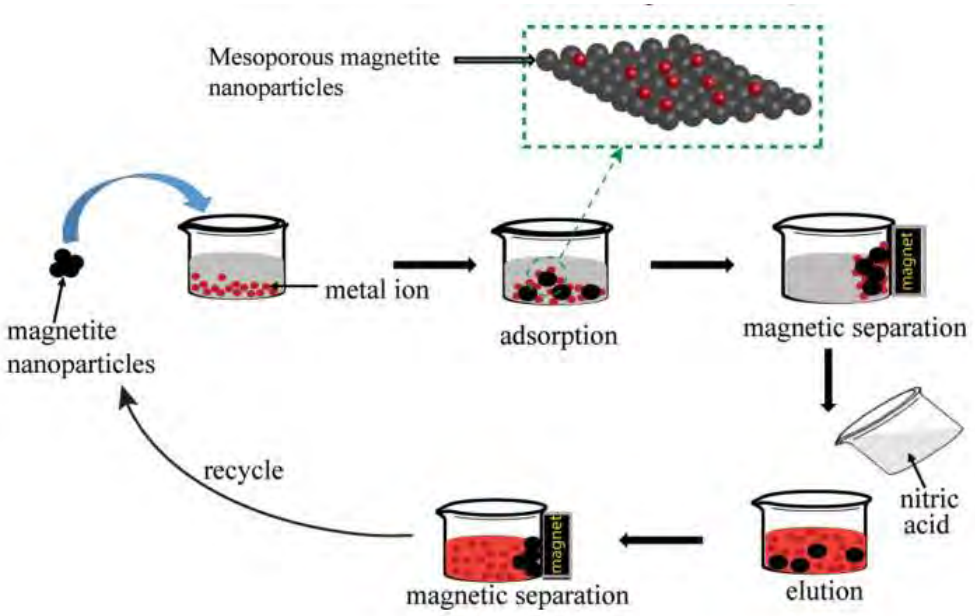

Figure 7 Adsorptive removal of heavy metals followed by desorption process

All of adsorption experiments were performed in duplicates and the metal ion concentration in control and final solutions was determined through inductively coupled plasma, optical emission spectroscopy (ICP-OES). The adsorption capacity (q_e, $mmolg^{-1}$) and the removal efficiency (α, %) were calculated using the following formula respectively

$$q_e = \left(\frac{C_o - C_e}{m}\right) . V$$

$$\alpha = \frac{C_o - C_e}{C_o} . 100$$

Where m = mass od adsorbent (g)

V = volume of solution (L)

C_o = initial concentration of the metal

C_e = equilibrium concentration of the metal

2.5. Adsorption Kinetics

The rate of solute uptake at given conditions such as pH, concentration or dose is described through the study of adsorption kinetics[108]. A kinetic model aids in the investigation of adsorption rates, models the process, and predicts adsorbent/adsorbate interaction[109] (physisorption or chemisorption). The weak physical forces, also known as Van der Waals forces, are generally involved in a physical adsorption process. On the contrary, strong bonding within the molecules of solute and adsorbent are formed during the chemical adsorption process[110]. The kinetics of Ni, Co, Cd and Cu adsorption on $MgFe_2O_4$ and $MgFe_2O_4$/AC was studied through pseudo first order and pseudo second order kinetics mechanism. The nonlinear form of pseudo first order and pseudo second order can be respectively represented as follows.

$$\boldsymbol{Q_t = Q_e(1 - e^{-k_1 t})}$$

$$\boldsymbol{Q_t = \frac{k_2 Q_e^2 t}{1 + k_2 Q_e t}}$$

Where K_1 = rate constant for pseudo first order kinetics

K_2 = rate constant for pseudo second order kinetics

Q_e (mg/g) = amount adsorbed at equilibrium

Q_t (mg/g) = amount adsorbed at time 't'

In addition to these, Elovich and intraparticle diffusion models were also applied.

2.6. Adsorption Isotherms

Adsorption isotherms are applied to study adsorption systems. For this purpose, equilibrium data is analyzed using a range of model isotherms for adsorption[111]. The equilibrium data for the Ni (II), Co (II), Cu (II), and Cd (II) removal process employing $MgFe_2O_4$/ AC in the present study were examined using Langmuir, Freundlich, Temkin and Dubinin Radushkevich (D-R) isotherm models. Nonlinear forms of all four adsorption models were applied.

Langmuir Isotherm

The Langmuir isotherm presupposes uniform monolayer coverage at homogenous sites on the adsorbent's surface. After saturation, no more adsorption can occur at this location and there is no interaction between molecules that have been adsorbed[111]. The nonlinear form of Langmuir isotherm is given as[36]

$$\boldsymbol{q_e = \frac{q_m K_L C_e}{1 + K_L C_e}}$$

Where C_e (mgg^{-1}) = concentration of adsorbate at equilibrium

K_L (mgg^{-1}) = Langmuir constant related to adsorption capacity

Freundlich Isotherm

The Freundlich isotherm applies to both, physisorption i.e., multilayer adsorption and chemisorption i.e., monolayer adsorption and assumes that surface of the adsorbent is heterogeneous with a non-uniform distribution of heat of adsorption over the adsorbent surface[36]. Freundlich isotherm is expressed as[36]

$$\boldsymbol{q_e = K_F C_e^{1/n}}$$

Where K_F (Lmg^{-1}) = adsorption capacity

$1/n$ = adsorption intensity

It also indicates the heterogeneity and relative distribution of the energy of the adsorbate sites[112].

Temkin Isotherm

The Temkin isotherm model considers how indirect adsorbate/adsorbate interactions affect the process of adsorption. Temkin isotherm is applicable only for an intermediate range of ionic concentration. Temkin isotherm is expressed as[112]

$$q_e = \frac{RT}{b}\ln(AC_e)$$

Where b = Temkin constant

Dubinin Radushkevich Isotherm

The D-R isotherm is expressed as

$$q_e = q_{D-R}e^{-K_{D-R}\varepsilon^2}$$

2.7. Regeneration Study of $MgFe_2O_4$ and $MgFe_2O_4$/AC

Exhausted adsorbent was added into nitric acid (pH = 1) and agitated at 150 rpm in a shaker at room temperature[113]. After 2 hours, the agitated adsorbent was separated from solvents, washed with water, and dried in hot air oven. Regenerated adsorbent was reused for adsorption of heavy metals to explore its reuse efficiency. Five consecutive cycles of adsorption-desorption reuse were performed and analyzed.

2.8. Characterization and Analytical Techniques

This section tells in-brief the basic principle, working and instrumentation of different characterization and analytical techniques which are required for this experiment to probe the properties and internal structure of the materials under study and to evaluate the adsorption capacity and removal efficiency of $MgFe_2O_4$ and $MgFe_2O_4$/ AC

2.8.1. Scanning Electron Microscopy (SEM) and Energy Dispersive X-ray Spectroscopy (EDS)

It is a device in which a high energy electron beam is used for imaging materials to study topography. SEM gives information about surface morphology and composition of the material under study[114].

It is based on the principle that the primary electrons are emitted by providing energy source to the sample's electrons. These electrons are then released as secondary electron. Electromagnetic lens focuses the electron beam on the surface of material. The diameter of the focused beam is up to 1nm. Secondary electrons, backscattered electrons and X-rays are produced because of this interaction. The number of detected electrons makes the image point brighter. SEM has a magnification ranging from 100-1000000X.

Specimen to be observed by SEM must satisfy certain parameters. It must be stable enough to withstand bombardment of high energy electron beams, it must be a good conductor of electrons. It must be clean and completely dry.

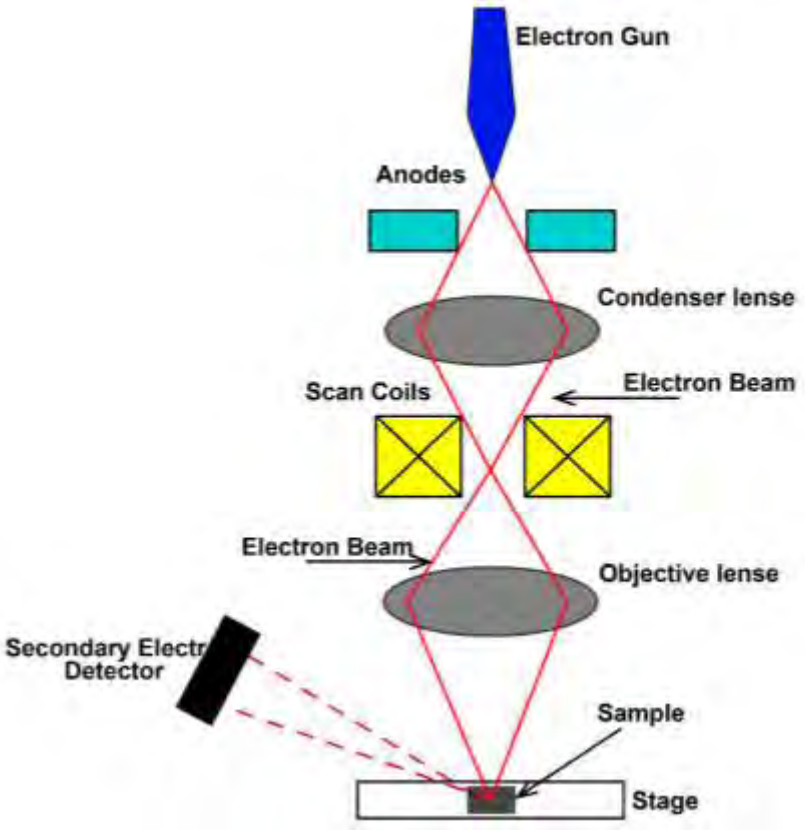

Figure 8 Schematic representation of working of SEM

2.8.3. Fourier Transform Infrared Spectroscopy

FTIR, or Fourier transform infrared is the preferrable technique for infrared spectroscopy. IR radiation is transmitted through a sample that absorbs part of the IR radiation, while transmitting the rest. The resulting spectrum creates a molecular fingerprint of the substance/ sample by representing its absorption and transmission. Just as no two unique molecular fingerprints ever match, no two unique molecular structures give the same IR spectrum. Because of this, IR spectroscopy can be used for several kinds of analysis. Furthermore, the size of the peak in the spectrum depicts the amount of material present[115].

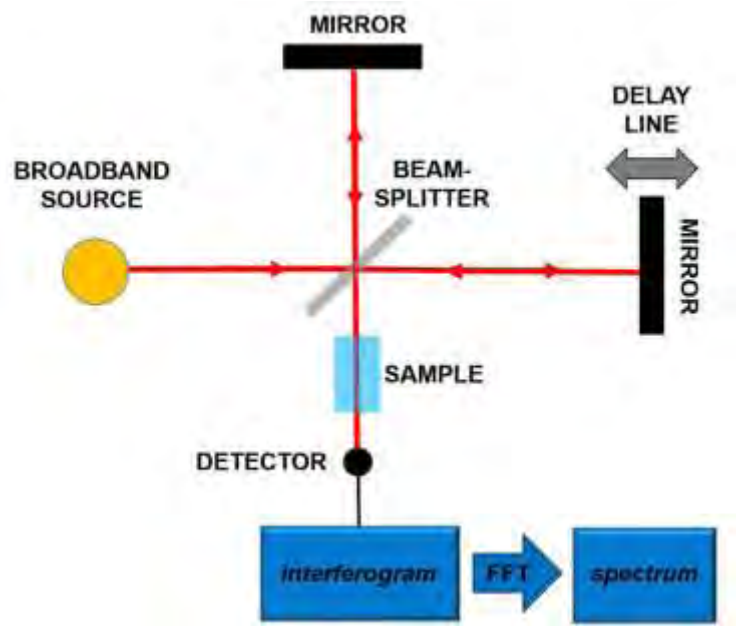

Figure 9 Schematic representation of working of FTIR

2.8.6. Inductively Coupled Plasma Optical Emission Spectroscopy

Inductively coupled plasma with optical emission spectrometry (ICP-OES), is one such method which can perform rapid and repeated elemental analyses with significantly greater sensitivity down to parts per million and parts per billion with significantly low interference. It is based on the spontaneous emission of photons from atoms or ions whose excitation occurs in a radio frequency discharge. Additionally, these photons have some distinctive energies that are primarily determined with the aid of a quantized level of energy. To compare with other spectrometric techniques, it is a versatile and sensitive method with lower detection limits, fewer chemical interferences, and a quicker processing time that yields precise and accurate findings[116].

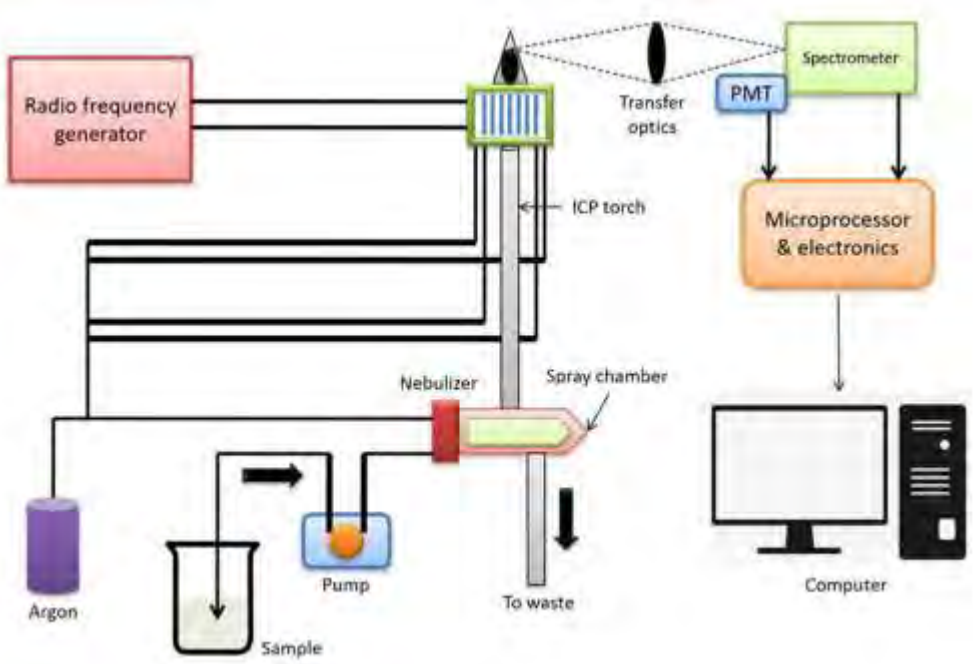

Figure 10 Schematic representation of working of ICP-OES

3. RESULTS AND DISCUSSION

This chapter includes all the results obtained from different characterization and analytical techniques after performing the experiments. As prepared $MgFe_2O_4$/ AC nanocomposite was characterized by studying their properties using SEM/ EDS, and FTIR. The adsorption capacity of the synthesized adsorbent for the removal of Ni (II), Co (II), Cu (II) and Cd (II) ions was studied using ICP-OES.

3.1. Characterization of $MgFe_2O_4$/ AC

3.1.1. Scanning Electron Microscopy/ Energy Dispersive X-ray Spectroscopy

SEM/ EDS of the synthesized $MgFe_2O_4$/ AC nanocomposite was performed to study the surface morphology, size, and elemental composition of the synthesized nanoparticles.

Given below are the SEM images and EDS $MgFe_2O_4$/ AC that show the presence of magnesium, iron, oxygen, and carbon in $MgFe_2O_4$/ AC. As per the EDS analysis there are also some minor elements present in the compound as impurities.

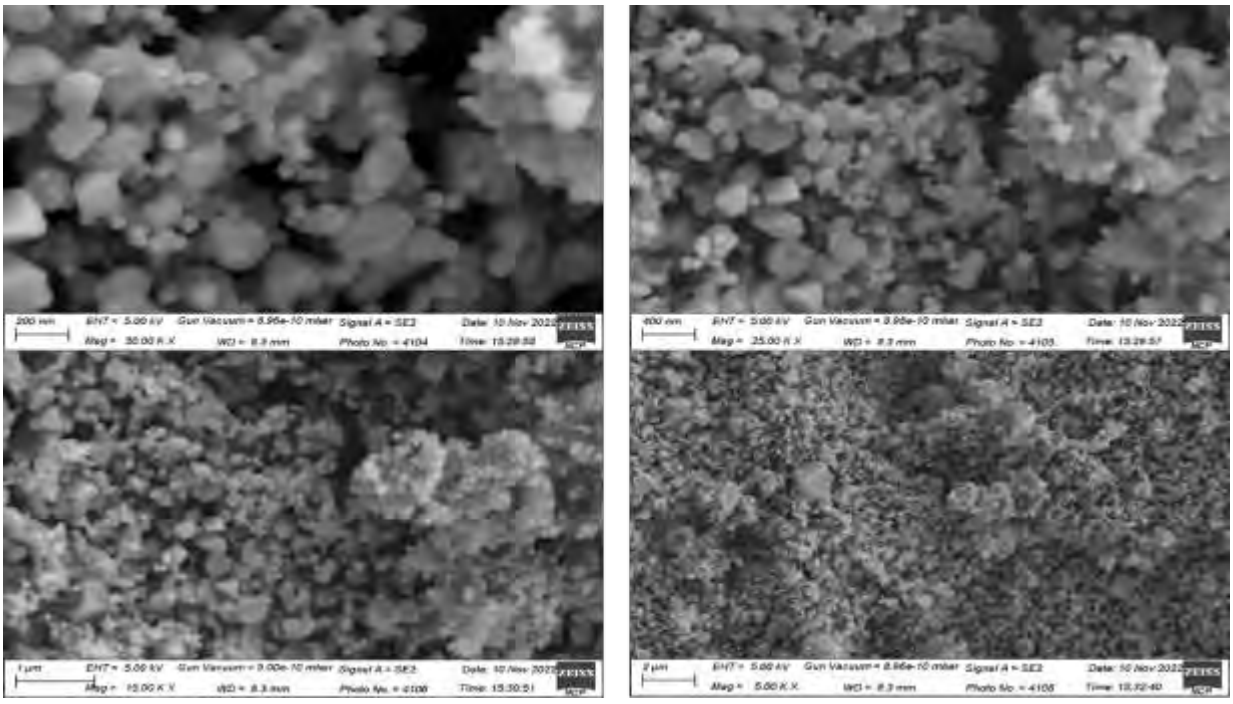

Figure 11 SEM images of MgFe2O4/ AC synthesized by coprecipitation method

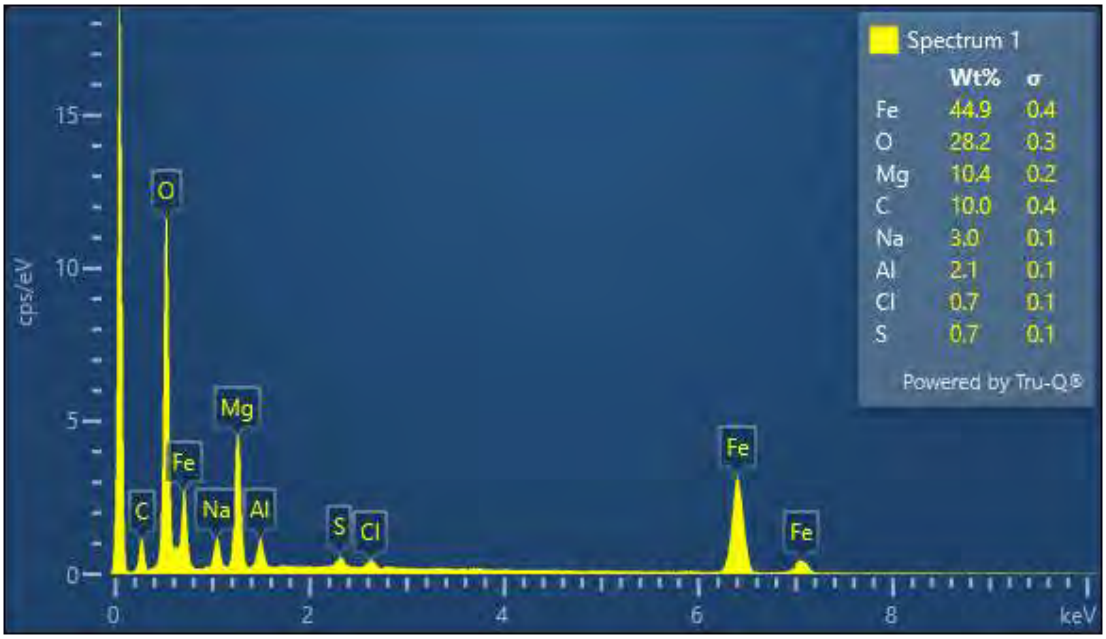

Figure 12 EDS of synthesized $MgFe_2O_4$/ AC

Because of its magnetic properties and the combining of primary particles held together by weak physical interactions such the van der Waals forces, the images reveal significant ferrite particle agglomeration. Furthermore, the surface morphology's high porosity is visible in the SEM images as also reported by Kurian et al in their synthesis of $CoFe_2O_4$ nanoparticles[42].

The SEM images of present study are similar to those present in a study conducted by Kaur et al in which $MgFe_2O_4$ nanoparticles and $MgFe_2O_4$/ AC nanocomposite were synthesized[27]. In the absence of any surfactant coating or functionalization, nanoparticles form clusters, demonstrating the inherent ability of pure magnetic nanoparticles to agglomerate. The flaky structure of amorphous carbon, which prevents clustering of NPs by limiting their binding with one another and hence improves the accessible surface area of NPs, is evident in the SEM picture of nanocomposite.

The EDS mapping of $MgFe_2O_4$/ AC shows the presence of relevant elements in the synthesized adsorbent. The determined percentage weight of Mg, Fe, O and C for $MgFe_2O_4$/ AC is 10.4%, 44.9%, 28.2% and 10% respectively. Although the structural

composition is heterogenous it is expected to contribute to increased active sites for adsorption as also reported in the EDS results of $MnFe_2O_4$/ biochar nanocomposite[43].

3.1.2. Fourier Transform Infrared Spectroscopy (FTIR)

The characteristic peaks for spinel ferrites are in the range of 400-600 cm^{-1} in infrared spectroscopy[42]. As depicted in the FTIR spectra of $MgFe_2O_4$/ AC given below, two sharp high frequency bands are present in the region between 500-600 cm^{-1} that shows the Fe-O bond and Mg-O bond, both of which indicate the ferrite phase. Absorption bands observed within this limit reveal the formation of single-phase spinel structure having tetrahedral (A) site and octahedral (B) sites in the lattice. The absorption band ν_1 is caused by the stretching vibrations of the tetrahedral metal (Fe^{3+})–oxygen bond, and the absorption band ν_2 is caused by the octahedral metal (Mg^{2+})–oxygen vibrations in octahedral sites.

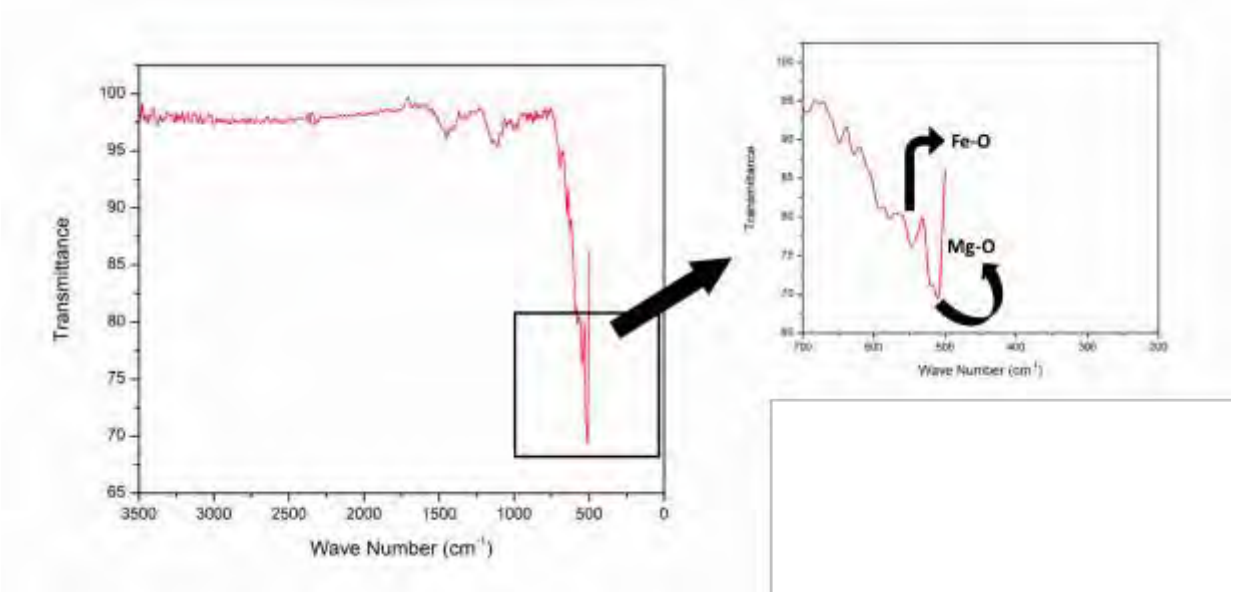

Figure 13 FTIR of $MgFe_2O_4$/ AC showing the presence of Mg-O and Fe-O bond

3.2. Adsorption Study

To determine the adsorption capacity and removal efficiency of $MgFe_2O_4$/ AC, batch adsorption experiments were performed, and different parameters were studied. The effect of each parameter was evaluated using inductively coupled plasma optical emission

spectroscopy (ICP-OES) by determining the metal ions concentration in each sample before and after adsorption.

3.2.1. Effect of Contact Time

The effect of contact time on the adsorption of metal cations was studied by performing adsorption experiments for 15, 30, 45, 60, 90, 120, 150 and 180 minutes for $MgFe_2O_4$/ AC. Metal ions concentration was determined through ICP-OES. The results obtained depicted that the adsorption of metal cations increased with increasing the contact time up to a certain point, after which there was no notable change in adsorption capacity or removal efficiency. Similar behavior has been reported for the removal of Mn (II), Co (II), Ni (II) and Cu (II) using $MgFe_2O_4$ as the nanoadsorbent[34] and for the simultaneous removal of Pb (II), Cd (II), Cu (II) and Ni (II) in river water using ultrafine magnetic Fe_3O_4 nanoparticles[44]. The constant removal rate after a certain period shows that reaction equilibrium has been achieved and the reaction has become independent of time i.e., increasing the time further does not increase the rate of adsorption.

Figure 4 shows the effect of time on the removal efficiency of $MgFe_2O_4$/ AC to remove the metal ions under study. The adsorption of each heavy metal ion increases with increasing time until 90 minutes for Cu (II), Cd (II), Co (II) and Ni (II) after which it achieves equilibrium and becomes constant. However, 97% copper was removed in the first 15 minutes of the reaction.

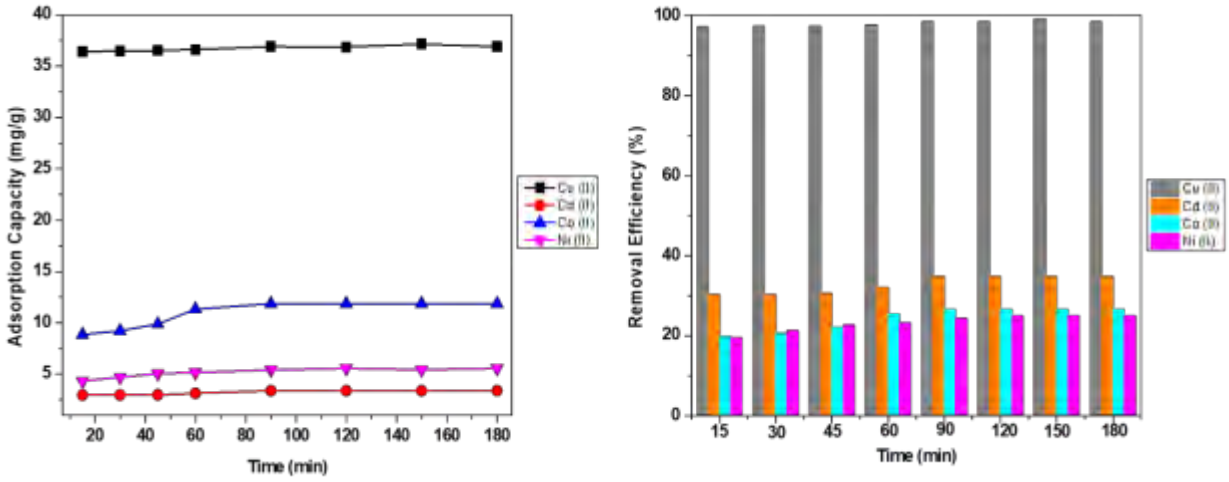

Figure 14 Adsorption capacity and removal efficiency of $MgFe_2O_4$/AC at 15, 30, 45. 60. 90. 120. 150 and 180 minutes

3.2.2. Effect of Adsorbent Dose

The adsorption was studied at 30mg, 50mg, 70 mg, 100mg, 150mg, 200mg and 250mg for 30 ml of the metal solution. It was observed that the removal of metals increased with increasing the dose of $MgFe_2O_4$/ AC as the number of available active sites increased for adsorption. However, adsorption capacity decreases as the dose increases because of the increase in the number of unsaturated sites. Between 30mg to 250mg the adsorption capacity decreased from 98.45mg/g to 12.17mg/g for Cu (II), from 4.12mg/g to 2.53mg/g for Cd (II), from 15.26mg/g to 13.12mg/g for Co (II), and from 7.94mg/g to 6.24mg/g. It was observed that at remarkably high adsorbent dose of 200 and 250mg per 30 ml, almost 99% of all four of the metal cations were removed. However, at dose up to 100mg, the removal of copper was comparatively greater than the removal of cadmium, cobalt, and nickel.

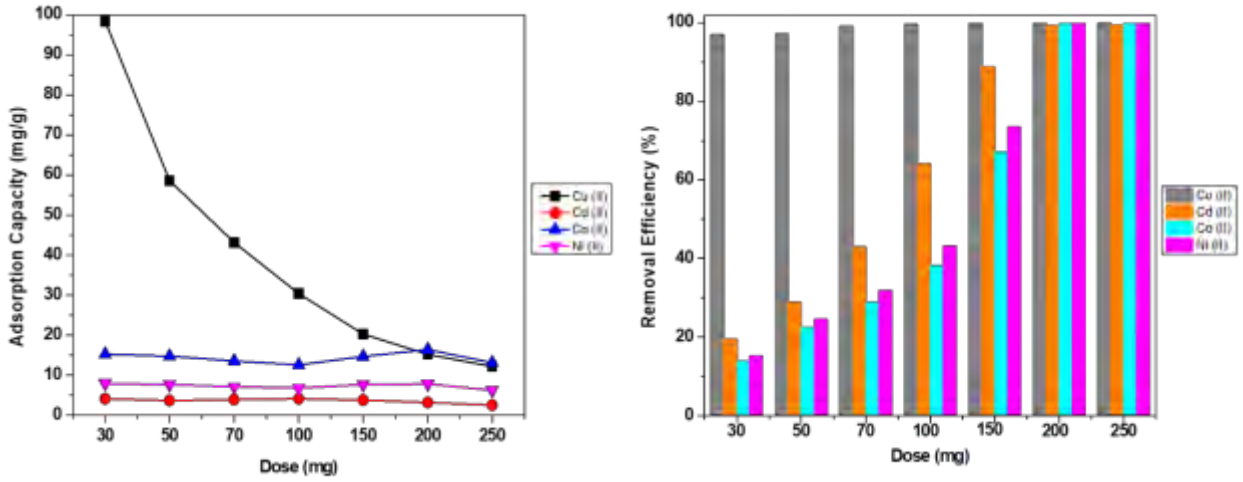

Figure 15 Adsorption capacity and removal efficiency of $MgFe_2O_4$/AC at 30mg, 50mg, 70mg, 100mg, 150mg, 200mg and 250mg adsorbent dose

3.2.3. Effect of Pollutant Concentration

As the concentration of pollutants increases for a fixed amount of adsorbent, the removal efficiency decreases. In the case of $MgFe_2O_4$/ AC, the removal efficiency for Cu (II) changed from 99% to 84%, for Cd (II) from 99% to 21%, for Co (II) 98% to 15%, and for Ni (II) it dropped from 99% to 3% as the concentration of each metal increased from 25ppm to 200ppm. Due to more adsorption, with increase in pollutant concentration the adsorption capacity increases for each metal because of saturation of active sites at the adsorbent surface. For Cu (II) an increase in the adsorption capacity was observed from 9mg/g to 85mg/g between 25ppm and 200ppm concentration. A similar trend was followed by Cd whose adsorption capacity increased from 2.68mg/g to 4.68mg/g. In the case of Co (II) and Ni (II) the adsorption capacity increased from 12.48mg/g to 19.55mg/g and 6.16mg/g to 12.43mg/g, respectively.

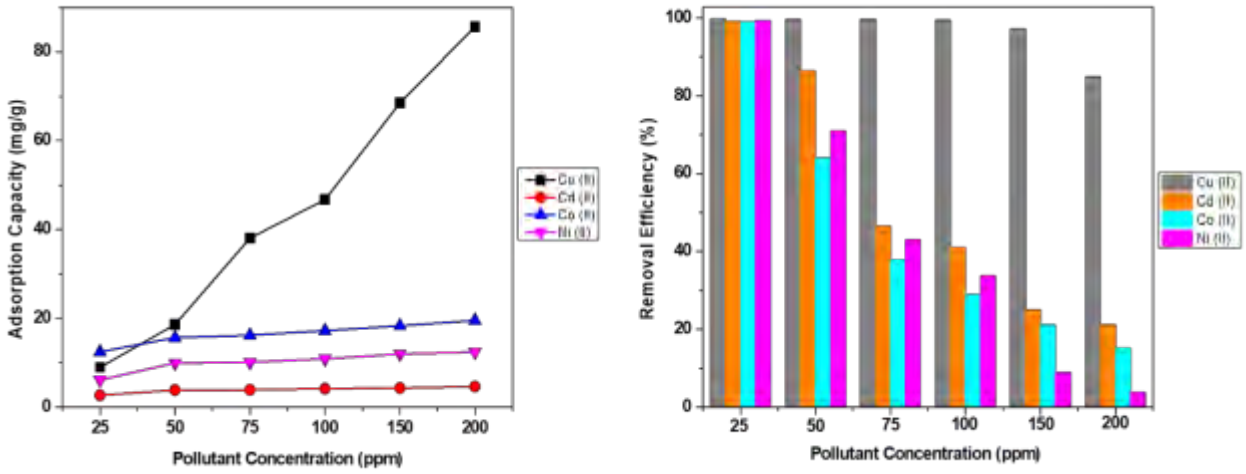

Figure 16 Adsorption capacity and removal efficiency of MgFe2O4/AC at 25ppm, 50ppm, 75ppm, 100ppm, 150ppm and 200ppm concentration of metal ions

3.2.4. Effect of pH

The experiments were performed at pH 1, 3, 5, 7 and 9 to study the effect of pH. The pH of a solution usually impacts the surface properties of the adsorbent and the degree of ionization of the adsorbate. The adsorption of the metals increased with the increase in the pH. The very low removal of metals at pH 1 and pH 3 could be because of the presence of H_3O^+ ions in the sample solutions. The hydronium ions compete with the metal cations for adsorption because of which the adsorption at these two pH values is low. At pH 5, the removal efficiency of Cu (II) was 98% and for Cd (II), Co (II), and Ni (II) was 22%, 20% and 29% respectively which is in accordance with the adsorption experiments performed earlier. At pH 7 the Cu (II) ions precipitate out as copper hydroxide and hence the removal efficiency of the Cd (II), Co (II) and Ni (II) increases to 79%, 72% and 71% respectively. However, at pH 9 all three of the metals precipitate out and hence adsorption did not occur.

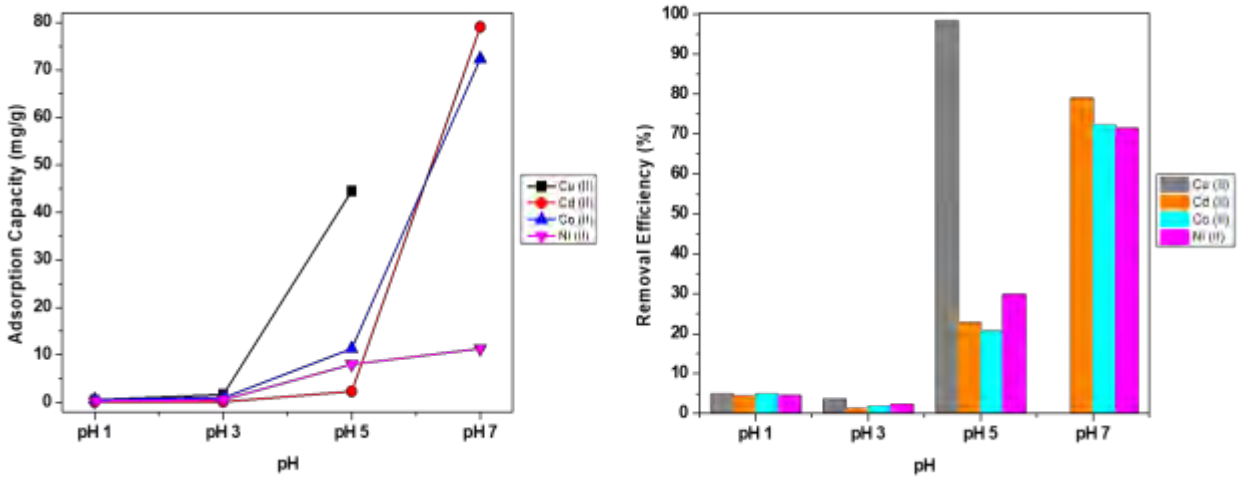

Figure 17 Adsorption capacity and removal efficiency of MgFe2O4/ AC at pH 1, 3, 5 and 7

3.2.5. Selective Adsorption of Cu (II)

In all the adsorption experiments performed, it was observed that the removal efficiency of Cu (II) was between 98% to 99% at optimum conditions as compared to the removal of other cations which were adsorbed in significantly low amount. To understand the affinity of the nanocomposite towards Cu (II), an interference study was done in the absence of copper. For this purpose, an adsorption experiment was performed using 50mg and 70mg of $MgFe_2O_4$/ AC, for 100ppm metal solution containing Cd (II), Co (II) and Ni (II). The results showed that in the absence of Cu (II) the removal of Cd (II), Co (II) and Ni (II) significantly increased from 28%, 22% and 24% to 57%, 59% and 61% respectively at 50mg and from 43%, 28%, 31% to 76%, 84%, and 83% respectively at 70mg dose of the nanocomposite. This is also aligned with the increased removal efficiency of Cd (II), Co (II) and Ni (II) at pH 7 after Cu (II) ions precipitated out from the solution. However, another experiment performed with a solution containing only Cu(II) again showed 99% removal of copper which means that $MgFe_2O_4$/AC has a greater affinity for copper. Although in the absence of copper, the removal efficiency of other metal ions increases, the removal efficiency of Cu (II) remains constant in all the experiments performed simultaneously and individually showing that $MgFe_2O_4$/AC can be used to selectively remove copper from a solution.

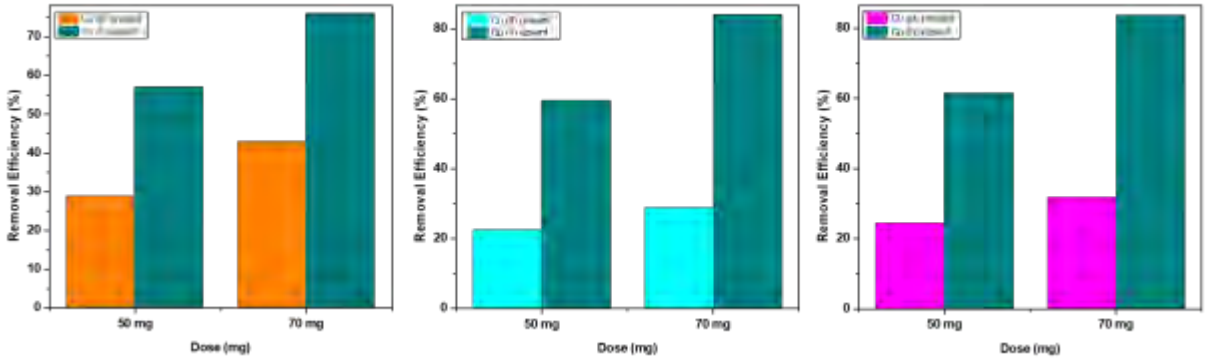

Figure 18 Removal efficiency of (a) Cd (II), (b) Co (II), and (c) Ni (II) in the presence and absence of Cu (II)

3.3. Adsorption Kinetics

Pseudo first order, pseudo second order, intraparticle diffusion and Elovich models were applied to understand the kinetics of the reaction. Nonlinear models were fitted in OriginPro 8.5, and the accuracy of fitting was analyzed using correlation coefficient (R^2). The model fittings for all the four models are presented in the graphs below:

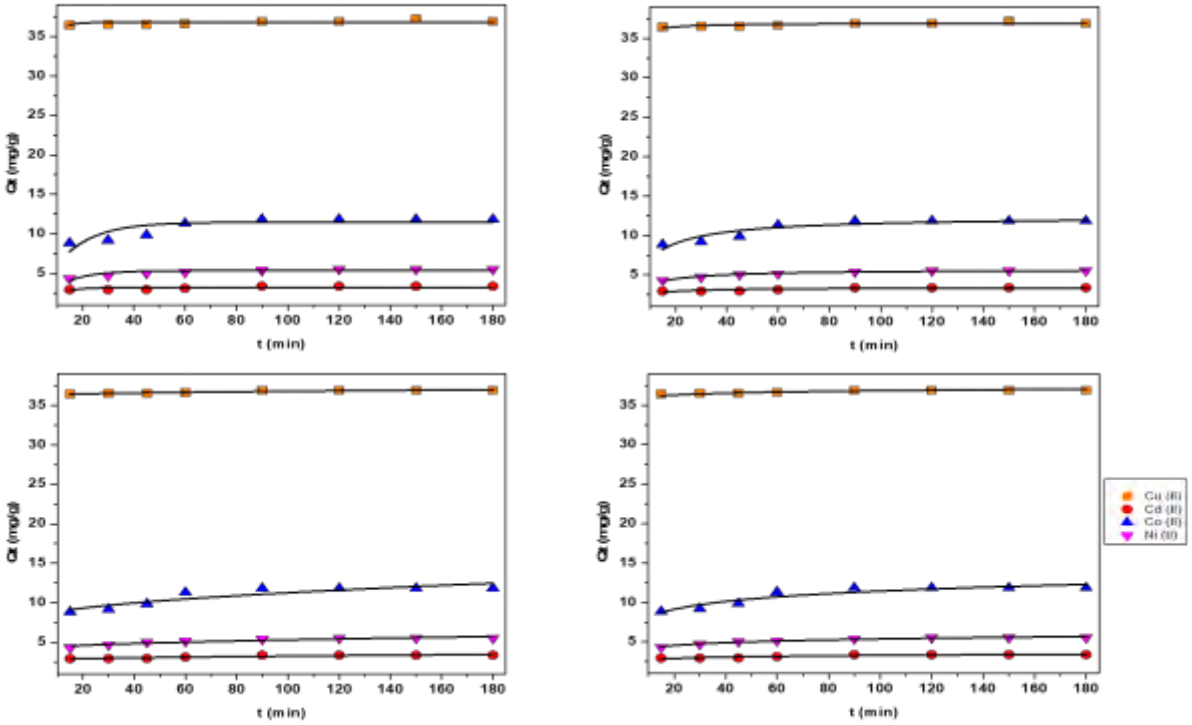

Figure 19 (a) Pseudo first order (b) pseudo second order (c) intraparticle diffusion (d) Elovich kinetic models for Cu (II), Cd (II), Co (II) and Ni (II)

The R^2 values and the respective parameters for each metal cation in all the four kinetic models are presented below.

Table 4 Kinetic models parameters for Cu (II), Cd (II), Co (II) and Ni (II)

	Pseudo First Order			Pseudo Second Order			Intraparticle Diffusion			Elovich		
	R^2	Q_e (mgg^{-1})	K_1	R^2	Q_e (mgg^{-1})	K_2 ($gmg^{-1}min^{-1}$)	R^2	K_d (mgg^{-1})	C	R^2	α (mg $^{1}min^{-1}$)	β g^{-1}(mgg^{-1}min^{-1})
Cu (II)	0.13	36.795	0.305	0.56	36.964	0.097	0.86	0.059	36.195	0.62	2.868	2.8E43
Cd (II)	0.16	3.249	0.145	0.62	3.405	0.092	0.83	0.059	2.68	0.81	4.318	3485.6
Co (II)	0.56	11.502	0.075	0.83	12.424	0.011	0.79	0.351	7.774	0.86	0.696	41.527
Ni (II)	0.68	5.362	0.097	0.958	5.702	0.033	0.87	0.126	4.059	0.96	1.927	164.74

The empirical pseudo first order model assumes that the rate of adsorption is directly proportional to the difference between the initial concentration of the heavy metal and the concentration at a given time during the adsorption process. The insignificant values of R^2

value for pseudo first order kinetics model indicate that this model is unable to explain the adsorption process using this assumption.

For Cu (II) and Cd (II) intraparticle diffusion model has the best fitting as the R^2 value is 0.86 and 0.83 for both respectively. The intraparticle diffusion model assumes that the rate limiting step in adsorption is the diffusion of the adsorbate from the solution into the pores of the adsorbent. When the value of C is zero, intraparticle diffusion is said to be the only rate determining step. On the other hand, when the value of $C \neq 0$, intraparticle diffusion is not solely responsible for the reaction kinetics and some other factors are also involved. The model indicates that for both Cu (II) and Cd (II) adsorption is occurring by diffusion at the pores. However, the value of $C \neq 0$ for both the metal cations indicating that adsorption mechanism cannot be explained only through intraparticle diffusion.

The Elovich model is suitable for heterogenous adsorbing surfaces and is satisfied in case of chemisorption. The correlation coefficient for Co (II) and Ni (II) is 0.86 and 0.96 respectively showing the accuracy of Elovich model for both the cations. In addition, the value of R^2 is 0.958 in case of pseudo second order kinetic model for Ni (II). A minimal difference between the R^2 values for both Elovich and pseudo second order for Ni (II) shows heterogenous chemisorption as pseudo second order is also satisfied for chemisorption. The value of β tells the desorption rate for Cd (II) and Ni (II).

3.4. Adsorption Isotherms

Nonlinear Freundlich, Langmuir, Temkin and Dubinin Radushkevich isotherm models were applied, and the accuracy of fitting was determined by correlation coefficient. The parameters for each isotherm models were also determined.

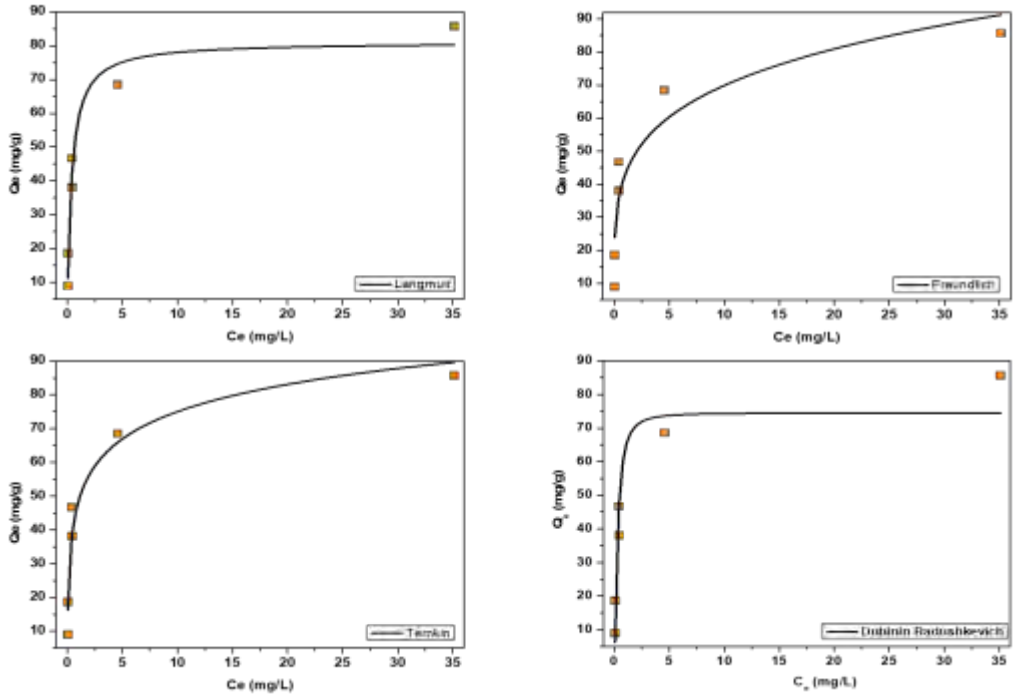

Figure 20 Freundlich, Langmuir, Temkin and D-R isotherm models for Cu (II)

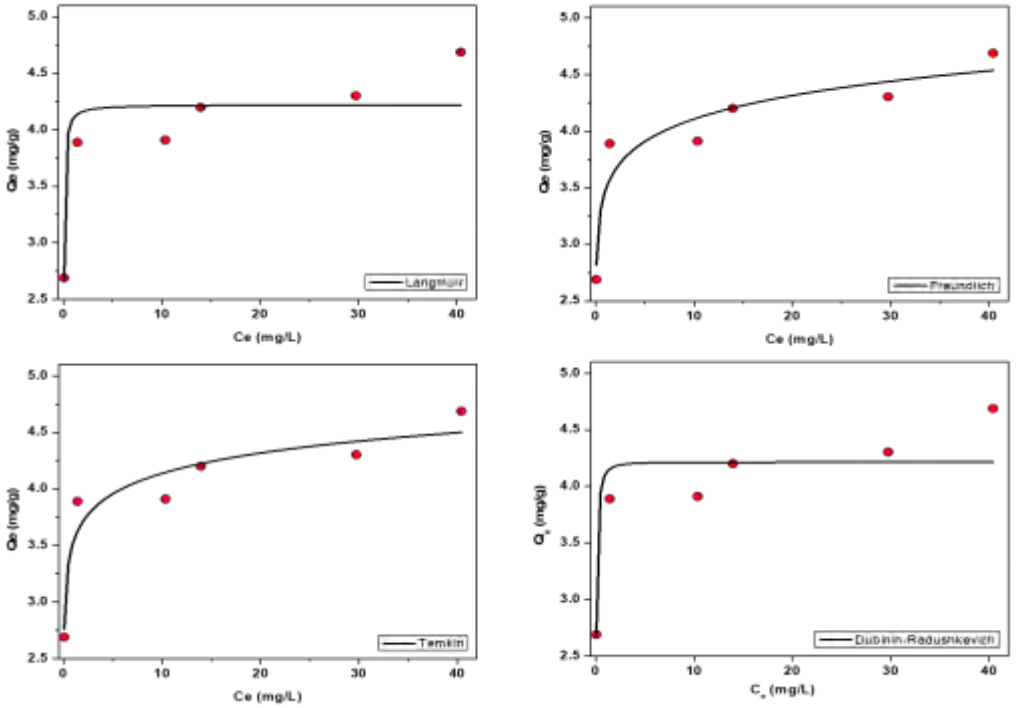

Figure 21 Freundlich, Langmuir, Temkin and D-R isotherm models for Cd (II)

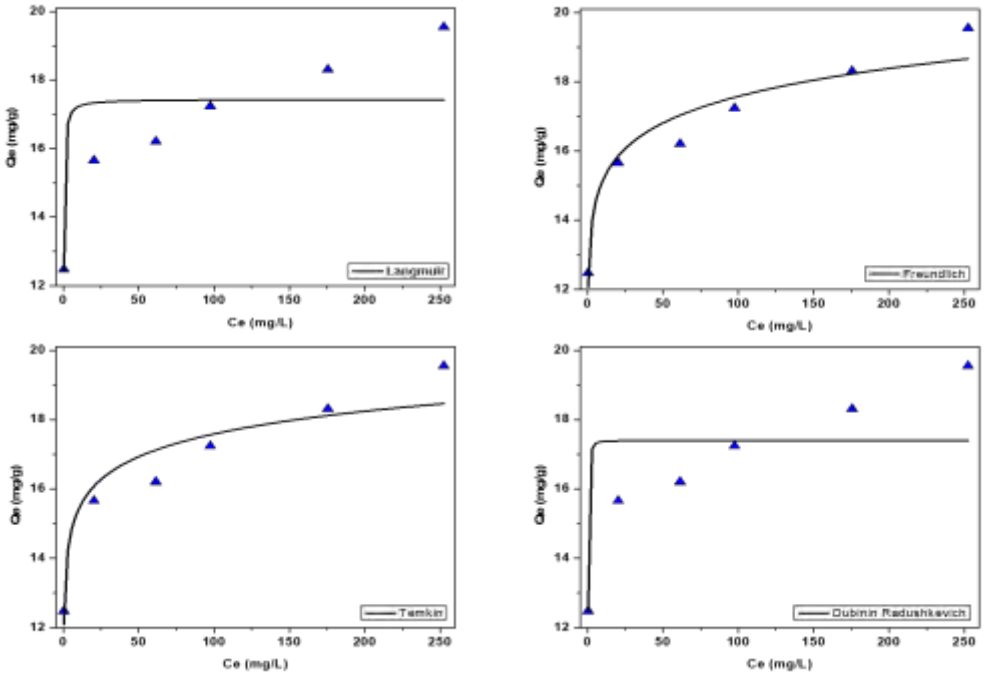

Figure 22 Freundlich, Langmuir, Temkin and D-R isotherm models for Co (II)

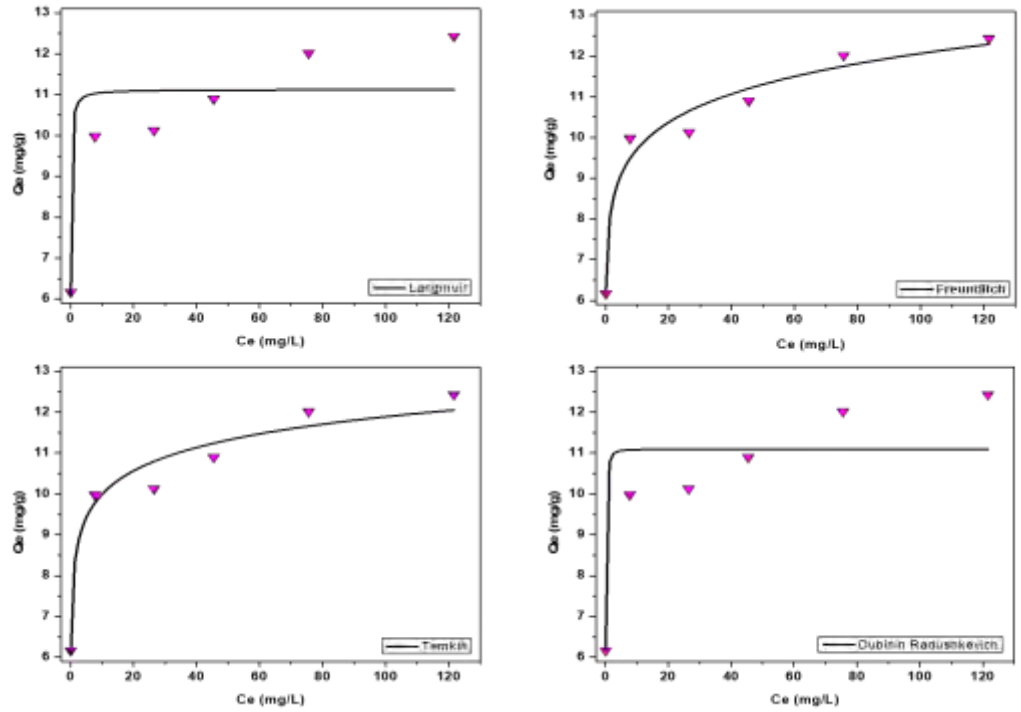

Figure 23 Freundlich, Langmuir, Temkin and D-R isotherm models for Ni (II)

The table below shows the R^2 and other parameter values of each model.

Table 5 Adsorption isotherm parameters for Cu (II), Cd (II), Co (II) and Ni (II)

	Langmuir			Freundlich			Temkin			D-R		
	R^2	Q_{max} (mg g^{-1})	K_L	R^2	n	K_F (mg g^{-1})	R^2	B (kcalmol^{-1})	A (L mg^{-1})	R^2	Q_D (mg g^{-1})	E (kJ g^{-1})
Cu (II)	0.949	81.126	2.495	0.85	0.212	42.838	0.95	0.002	62.659	0.88	74.524	0.317
Cd (II)	0.79	4.225	34.178	0.89	0.071	3.486	0.90	6×10^{-4}	83×10^{6}	0.78	4.213	0.049
Co (II)	0.60	17.440	8.264	0.93	0.065	13.057	0.89	2×10^{-3}	1×10^{6}	0.58	17.396	0.154
Ni (II)	0.77	11.127	14.411	0.96	0.094	7.832	0.95	2×10^{-3}	18×10^{3}	0.76	11.092	0.091

The strong correlation suggests that both the Temkin and Langmuir isotherms are appropriate representations of the adsorption process in case of Cu(II). The Langmuir model provides information regarding adsorption at homogenous active sites.

The obtained Temkin constant for Cu(II), B, is 0.002 kcal/mol. This parameter is related to the heat of adsorption, and its value indicates the strength of the adsorbate-adsorbent interaction. A low value of B suggests a weaker adsorbate-adsorbent interaction. In the case of Cu(II), a low B value implies that the adsorption process may involve weaker interactions, such as van der Waals forces. The value of parameter A is associated with the adsorption capacity and reflects the surface heterogeneity and available active sites on the adsorbent material. A higher A value indicates a larger adsorption capacity and suggests that the $MgFe_2O_4$/AC nanocomposites possess a significant number of active sites for heavy metal adsorption.

An accurate fitting of both Langmuir and Temkin model makes it difficult to accurately predict and adsorption mechanism for the selective adsorption of Cu (II).

For Cd (II) the R^2 value shows an accurate fitting of both Freundlich and Temkin model as the R^2 values are 0.90 and 0.89 respectively. Based on the data we can predict that a multilayer adsorption occurred at heterogeneous sites of the adsorbent. In the case of Co (II) and Ni (II), Freundlich model best fits showing that there is multilayer heterogenous adsorption which aligns with the Elovich model for chemical adsorption at heterogeneous surfaces.

3.5. Proposed Mechanism

Based on the data obtained from adsorption isotherms and adsorption kinetics, it can be proposed that $MgFe_2O_4$/AC has heterogenous sites for adsorption as explained by the fitting of Freundlich, Temkin isotherm and Elovich kinetics model. Cu (II) was removed via physical adsorption through Van der Waal forces as proposed by the fitting of Temkin isotherm model, and through monolayer chemical adsorption at homogenous sites as proposed by Langmuir model. In the case of Cd (II) the accurate fitting of Freundlich model, Temkin model and intraparticle diffusion model propose that the removal of Cd (II) occurred through physisorption and through diffusion at pores. Lastly, Ni (II) and Co (II) followed multilayer chemisorption and physisorption at heterogenous surfaces as explained by the fitting of Freundlich model and Elovich model. To conclude we can say that adsorption occurred in multiple ways in case of Cu (II), Co (II) and Ni (II) and followed physisorption in case of Cd (II).

The adsorption of Cu (II) at a monolayer homogenous surface could be the reason of its selective removal as compared to the removal of other metal cations.

3.6. Regeneration and Reusability

$MgFe_2O_4$/AC and other spinel ferrite nanoparticles and nanocomposites are reported to exhibit excellent regeneration and reusability properties. However, in this study there was a huge loss of MFNP nanocomposite during the regeneration and drying step which led to a decreased amount of adsorbent for every next reusability cycle. Because of this, the reusability of the adsorbent did not show satisfactory results and by the fifth cycle the removal efficiency had reduced from 99% to 7%, 52% to 6%, 30 percent to 3%, and 33% to 2% for Cu (II), Cd (II), Co (II) and Ni (II) respectively. The adsorption capacity also decreased from 49mg/g to 3mg/g, 6mg/g to 0.8mg/g, 16mg/g to 1.7mg/g, 9mg/g to 0.61mg/g for Cu (II), Cd (II), Co (II) and Ni (II) respectively.

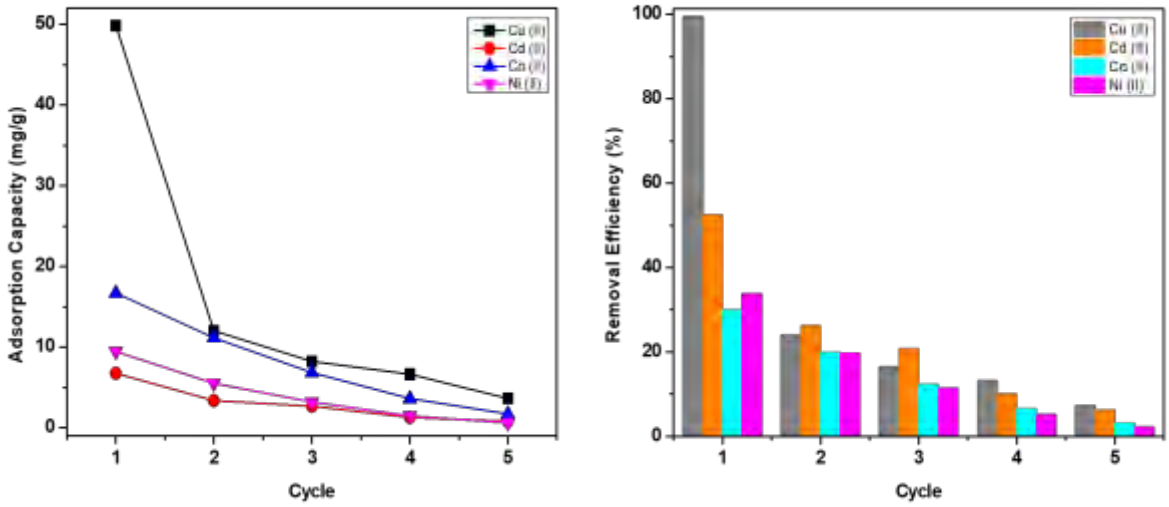

Figure 24 Adsorption capacity and removal efficiency of MgFe2O4/ AC after 5 consecutive regeneration and reusability cycle

3.7. Comparison with Other Studies

Table 6 shows a comparison of the reported work for the removal of different heavy metals using spinel ferrites and spinel ferrite nanocomposites and the removal of heavy metals using magnesium ferrite/ activated carbon in this study.

Table 6 Comparison of adsorption capacity and removal efficiency between reported work and the present study

Spinel Ferrite	**Target Metal**	**Adsorption Capacity/ Removal Efficiency (%)**	**Ref.**
Fe_3O_4	Pb (II), Cd (II), Cu (II), Ni (II)	86%, 80%, 84%, 54%	120
$MgFe_2O_4$	Mn (II), Co (II), Cu (II), Ni (II)	1.56 mmol/g, 2.30 mmol/g, 0.46 mmol/g, 0.89 mmol/g	107
$NiFe_2O_4$	Pb (II), Cd (II), Cr (II)	79%, 87%, 89%	121
$MnFe_2O_4$/ biochar	Pb (II), Cd (II), Cu (II)	34.36 mg/g, 0.84 mg/g, 14.96 mg/g	119
$CuFe_2O_4$	Cu (II), Ni (II), Zn (II)	83.5%, 98.8%, 99.8%	122
$MgFe_2O_4$/ GO	Pb (II), Ni (II)	143 mg/g, 100 mg/g	101
$MgFe_2O_4$	Co (II)	67.41 mg/g	64
$MgFe_2O_4$/ AC	Cu (II), Cd (II), Co (II), Ni (II) Cd (II), Co (II), Ni (II)	99%, 99%, 98%, 99% (25 ppm) 76%, 84%, 83% (70mg, without Cu (II))	Present study

CONCLUSION

The present study was conducted to see the application of magnesium ferrite/ activated carbon in wastewater treatment. $MgFe_2O_4$/ AC nanocomposite was synthesized by coprecipitation method and was confirmed by SEM/ EDS, and FTIR. The simultaneous adsorptive removal of Cu (II), Cd (II), Co (II) and Ni (II) ions from laboratory prepared samples was tested. The synthesized adsorbent had high adsorption capacity for Cu (II) ions as compared to Cd (II), Co (II) and Ni (II) as shown through different experiments. $MgFe_2O_4$/ AC showed a selective removal of Cu (II) in all experiments which was also proved by performing an experiment without copper ions in the solution. The adsorption of Cd (II), Co (II) and Ni (II) significantly improved in the absence of Cu (II) ions. The regeneration and reusability tests were performed. However, there was workup loss during the regeneration cycles which impacted the reusability of the adsorbent and the adsorption efficiency decreased with each cycle.

The study opens a new pathway for exploring the removal of copper using magnesium ferrite/ activated carbon nanocomposite at industrial scale and testing its application for the recovery and reuse of copper metal from different water sources. In addition, it also provides an opportunity to study the surface modification and addition of functional groups in magnesium ferrite/ activated carbon to improve its adsorption capacity for the removal of various heavy metals simultaneously.

REFERENCES

1. Yadav, D., Singh, P. & Kumar, P. Application of nanoparticles for inorganic water purification. in *Inorganic Pollutants in Water* 221–243 (Elsevier, 2020). doi:10.1016/b978-0-12-818965-8.00012-3.

2. Wing, S., Lowman, A., Keil, A. & Marshall, S. W. Odors from Sewage Sludge and Livestock: Associations with Self-Reported Health.

3. Altenburger, R. *et al.* Future water quality monitoring — Adapting tools to deal with mixtures of pollutants in water resource management. *Science of The Total Environment* **512–513**, 540–551 (2015).

4. Maryam, B. & Büyükgüngör, H. Wastewater reclamation and reuse trends in Turkey: Opportunities and challenges. *Journal of Water Process Engineering* **30**, 100501 (2019).

5. Lyu, S., Chen, W., Zhang, W., Fan, Y. & Jiao, W. Wastewater reclamation and reuse in China: Opportunities and challenges. *Journal of Environmental Sciences* **39**, 86–96 (2016).

6. Li, K. *et al.* Efficient adsorption of both methyl orange and chromium from their aqueous mixtures using a quaternary ammonium salt modified chitosan magnetic composite adsorbent. *Chemosphere* **154**, 310–318 (2016).

7. Gollavelli, G., Chang, C.-C. & Ling, Y.-C. Facile Synthesis of Smart Magnetic Graphene for Safe Drinking Water: Heavy Metal Removal and Disinfection Control. (2013) doi:10.1021/sc300112z.

8. Environmental Science and Technology Briefs for Citizens Human Health Effects of Heavy Metals.

9. Inglezakis, V. J., Loizidou, M. D. & Grigoropoulou, H. P. Equilibrium and kinetic ion exchange studies of Pb2+, Cr3+, Fe3+ and Cu2+ on natural clinoptilolite. *Water Res* **36**, 2784–2792 (2002).

10. Saif, M. M. S., Kumar, N. S. & Prasad, M. N. V. Binding of cadmium to Strychnos potatorum seed proteins in aqueous solution: Adsorption kinetics and relevance to water purification. *Colloids Surf B Biointerfaces* **94**, 73–79 (2012).

11. Roy, A. & Bhattacharya, J. *Nanotechnology in industrial wastewater treatment*.

12. Zhang, S., Cheng, F., Tao, Z., Gao, F. & Chen, J. Removal of nickel ions from wastewater by Mg(OH)2/MgO nanostructures embedded in Al2O3 membranes. *J Alloys Compd* **426**, 281–285 (2006).

13. Al-Asheh, S. & Duvnjak, Z. Sorption of cadmium and other heavy metals by pine bark. *J Hazard Mater* **56**, 35–51 (1997).

14. Srivastava, V., Sharma, Y. C. & Sillanpää, M. Application of nano-magnesso ferrite (n-MgFe 2 O 4) for the removal of Co 2+ ions from synthetic wastewater: Kinetic, equilibrium and thermodynamic studies. *Appl Surf Sci* **338**, 42–54 (2015).

15. Zhu, X., Song, T., Lv, Z. & Ji, G. High-efficiency and low-cost α-Fe2O3 nanoparticles-coated volcanic rock for Cd(II) removal from wastewater. *Process Safety and Environmental Protection* **104**, 373–381 (2016).

16. Reddy, S. A. *et al.* Extractive spectrophotometric determination of trace amounts of cadmium(II) in medicinal leaves and environmental samples using benzildithiosemicarbazone (BDTSC). *J Hazard Mater* **152**, 903–909 (2008).

17. Wadhawan, S., Jain, A., Nayyar, J. & Mehta, S. K. Role of nanomaterials as adsorbents in heavy metal ion removal from waste water: A review. *Journal of Water Process Engineering* vol. 33 Preprint at https://doi.org/10.1016/j.jwpe.2019.101038 (2020).

18. Razzaz, A., Ghorban, S., Hosayni, L., Irani, M. & Aliabadi, M. Chitosan nanofibers functionalized by TiO2 nanoparticles for the removal of heavy metal ions. *J Taiwan Inst Chem Eng* **58**, 333–343 (2016).

19. Fu, F. & Wang, Q. Removal of heavy metal ions from wastewaters: A review. *J Environ Manage* **92**, 407–418 (2011).

20. Smara, A., Delimi, R., Chainet, E. & Sandeaux, J. Removal of heavy metals from diluted mixtures by a hybrid ion-exchange/electrodialysis process. *Sep Purif Technol* **57**, 103–110 (2007).

21. Akbal, F. & Camci, S. Comparison of electrocoagulation and chemical coagulation for heavy metal removal. *Chem Eng Technol* **33**, 1655–1664 (2010).

22. Beltrán Heredia, J. & Sánchez Martín, J. Removing heavy metals from polluted surface water with a tannin-based flocculant agent. *J Hazard Mater* **165**, 1215–1218 (2009).

23. Chang, Q., Zhang, M. & Wang, J. Removal of Cu2+ and turbidity from wastewater by mercaptoacetyl chitosan. *J Hazard Mater* **169**, 621–625 (2009).

24. Chang, Q. & Wang, G. Study on the macromolecular coagulant PEX which traps heavy metals. *Chem Eng Sci* **62**, 4636–4643 (2007).

25. Murthy, Z. V. P. & Chaudhari, L. B. Application of nanofiltration for the rejection of nickel ions from aqueous solutions and estimation of membrane transport parameters. *J Hazard Mater* **160**, 70–77 (2008).

26. Muthukrishnan, M. & Guha, B. K. Effect of pH on rejection of hexavalent chromium by nanofiltration. *Desalination* **219**, 171–178 (2008).

27. Cséfalvay, E., Pauer, V. & Mizsey, P. Recovery of copper from process waters by nanofiltration and reverse osmosis. *Desalination* **240**, 132–142 (2009).

28. Ahmad, A. L. & Ooi, B. S. A study on acid reclamation and copper recovery using low pressure nanofiltration membrane. *Chemical Engineering Journal* **156**, 257–263 (2010).

29. Nguyen, C. M., Bang, S., Cho, J. & Kim, K. W. Performance and mechanism of arsenic removal from water by a nanofiltration membrane. *Desalination* **245**, 82–94 (2009).

30. Figoli, A. *et al.* Influence of operating parameters on the arsenic removal by nanofiltration. *Water Res* **44**, 97–104 (2010).

31. Belkacem, M., Khodir, M. & Abdelkrim, S. Treatment characteristics of textile wastewater and removal of heavy metals using the electroflotation technique. *Desalination* **228**, 245–254 (2008).

32. Singh, S., Kapoor, D., Khasnabis, S., Singh, J. & Ramamurthy, P. C. Mechanism and kinetics of adsorption and removal of heavy metals from wastewater using nanomaterials. *Environmental Chemistry Letters* vol. 19 2351–2381 Preprint at https://doi.org/10.1007/s10311-021-01196-w (2021).

33. El-sayed, M. E. A. Nanoadsorbents for water and wastewater remediation. *Science of the Total Environment* vol. 739 Preprint at https://doi.org/10.1016/j.scitotenv.2020.139903 (2020).

34. Wang, S., Boyjoo, Y., Choueib, A. & Zhu, Z. H. Removal of dyes from aqueous solution using fly ash and red mud. *undefined* **39**, 129–138 (2005).

35. Yadanaparthi, S. K. R., Graybill, D. & von Wandruszka, R. Adsorbents for the removal of arsenic, cadmium, and lead from contaminated waters. *undefined* **171**, 1–15 (2009).

36. Wang, J. & Guo, X. Adsorption isotherm models: Classification, physical meaning, application and solving method. *Chemosphere* **258**, 127279 (2020).

37. Tahoon, M. A., Siddeeg, S. M., Alsaiari, N. S., Mnif, W. & Ben Rebah, F. Effective heavy metals removal fromwater using nanomaterials: A review. *Processes* vol. 8 Preprint at https://doi.org/10.3390/PR8060645 (2020).

38. Kakavandi, B. *et al.* Pb(II) Adsorption onto a Magnetic Composite of Activated Carbon and Superparamagnetic Fe3O4 Nanoparticles: Experimental and Modeling Study. *Clean (Weinh)* **43**, 1157–1166 (2015).

39. Xu, P. *et al.* Adsorption of Pb(II) by iron oxide nanoparticles immobilized Phanerochaete chrysosporium: Equilibrium, kinetic, thermodynamic and mechanisms analysis. *Chemical Engineering Journal* **203**, 423–431 (2012).

40. Channegowda, M. Recent advances in environmentally benign hierarchical inorganic nano-adsorbents for the removal of poisonous metal ions in water: A review with mechanistic insight into toxicity and adsorption. *Nanoscale Advances* vol. 2 5529–5554 Preprint at https://doi.org/10.1039/d0na00650e (2020).

41. Rad, L. R. *et al.* Removal of Ni2+ and Cd2+ ions from aqueous solutions using electrospun PVA/zeolite nanofibrous adsorbent. *Chemical Engineering Journal* **256**, 119–127 (2014).

42. Shah, L. A. *et al.* Superabsorbent polymer hydrogels with good thermal and mechanical properties for removal of selected heavy metal ions. *J Clean Prod* **201**, 78–87 (2018).

43. Cegłowski, M., Gierczyk, B., Frankowski, M. & Popenda, Ł. A new low-cost polymeric adsorbents with polyamine chelating groups for efficient removal of heavy metal ions from water solutions. *React Funct Polym* **131**, 64–74 (2018).

44. Esmaeili, A. & Khoshnevisan, N. Optimization of process parameters for removal of heavy metals by biomass of Cu and Co-doped alginate-coated chitosan nanoparticles. *Bioresour Technol* **218**, 650–658 (2016).

45. Hallaji, H., Keshtkar, A. R. & Moosavian, M. A. A novel electrospun PVA/ZnO nanofiber adsorbent for U(VI), Cu(II) and Ni(II) removal from aqueous solution. *J Taiwan Inst Chem Eng* **46**, 109–118 (2015).

46. Hojamberdiev, M. *et al.* Ligand-immobilized spent alumina catalyst for effective removal of heavy metal ions from model contaminated water. *J Environ Chem Eng* **6**, 4623–4633 (2018).

47. Najafi, M., Yousefi, Y. & Rafati, A. A. Synthesis, characterization and adsorption studies of several heavy metal ions on amino-functionalized silica nano hollow sphere and silica gel. *Sep Purif Technol* **85**, 193–205 (2012).

48. Deravanesiyan, M., Beheshti, M. & Malekpour, A. The removal of Cr (III) and Co (II) ions from aqueous solution by two mechanisms using a new sorbent (alumina nanoparticles immobilized zeolite) — Equilibrium, kinetic and thermodynamic studies. *J Mol Liq* **209**, 246–257 (2015).

49. Morillo Martín, D., Faccini, M., García, M. A. & Amantia, D. Highly efficient removal of heavy metal ions from polluted water using ion-selective polyacrylonitrile nanofibers. *J Environ Chem Eng* **6**, 236–245 (2018).

50. Gao, J. *et al.* Single step synthesis of amine-functionalized mesoporous magnetite nanoparticles and their application for copper ions removal from aqueous solution. *J Colloid Interface Sci* **481**, 220–228 (2016).

51. Kotsyuda, S. S. *et al.* Bifunctional silica nanospheres with 3-aminopropyl and phenyl groups. Synthesis approach and prospects of their applications. *Appl Surf Sci* **420**, 782–791 (2017).

52. Li, Y. *et al.* Super rapid removal of copper, cadmium and lead ions from water by NTA-silica gel †. (2019) doi:10.1039/c8ra08638a.

53. Lo, I. M. C., Hu, J. & Chen, G. Iron-based magnetic nanoparticles for removal of heavy metals from electroplating and metal-finishing wastewater. *Nanotechnologies for Water Environment Applications* 213–268 (2009) doi:10.1061/9780784410301.CH09.

54. Khan, F. S. A. *et al.* Magnetic nanoparticles incorporation into different substrates for dyes and heavy metals removal—A Review. *Environmental Science and Pollution Research* vol. 27 43526–43541 Preprint at https://doi.org/10.1007/s11356-020-10482-z (2020).

55. Liu, J., Qiao, S. Z., Hu, Q. H. & Lu, G. Q. Magnetic Nanocomposites with Mesoporous Structures: Synthesis and Applications. *Small* **7**, 425–443 (2011).

56. Roeder, L., Bender, P., Tschöpe, A., Birringer, R. & Schmidt, A. M. Shear modulus determination in model hydrogels by means of elongated magnetic nanoprobes. *undefined* **50**, 1772–1781 (2012).

57. Gómez-Pastora, J., Bringas, E. & Ortiz, I. Recent progress and future challenges on the use of high performance magnetic nano-adsorbents in environmental applications. *Chemical Engineering Journal* vol. 256 187–204 Preprint at https://doi.org/10.1016/j.cej.2014.06.119 (2014).

58. Badruddoza, A. Z. M., Shawon, Z. B. Z., Tay, W. J. D., Hidajat, K. & Uddin, M. S. Fe3O4/cyclodextrin polymer nanocomposites for selective heavy metals removal from industrial wastewater. *Carbohydr Polym* **91**, 322–332 (2013).

59. Li, G., Zhao, Z., Liu, J. & Jiang, G. Effective heavy metal removal from aqueous systems by thiol functionalized magnetic mesoporous silica.

60. Saravanan, P., Vinod, V. T. P., Sreedhar, B. & Sashidhar, R. B. Gum kondagogu modified magnetic nano-adsorbent: An efficient protocol for removal of various toxic metal ions. *Materials Science and Engineering: C* **32**, 581–586 (2012).

61. Khan, F. S. A. *et al.* Magnetic nanoadsorbents' potential route for heavy metals removal—a review. *Environmental Science and Pollution Research* **27**, 24342–24356 (2020).

62. Liu, M., Chen, C., Hu, J., Wu, X. & Wang, X. Synthesis of magnetite/graphene oxide composite and application for cobalt(II) removal. *Journal of Physical Chemistry C* **115**, 25234–25240 (2011).

63. Chang, Y. C., Chang, S. W. & Chen, D. H. Magnetic chitosan nanoparticles: Studies on chitosan binding and adsorption of Co(II) ions. *React Funct Polym* **66**, 335–341 (2006).

64. Srivastava, V., Sharma, Y. C. & Sillanpää, M. Application of nano-magnesso ferrite (n-MgFe 2 O 4) for the removal of Co 2+ ions from synthetic wastewater: Kinetic, equilibrium and thermodynamic studies. *Appl Surf Sci* **338**, 42–54 (2015).

65. Roy, A. & Bhattacharya, J. Removal of Cu(II), Zn(II) and Pb(II) from water using microwave-assisted synthesized maghemite nanotubes. *Chemical Engineering Journal* **211–212**, 493–500 (2012).

66. Ahmed, M. A., Ali, S. M., El-Dek, S. I. & Galal, A. Magnetite–hematite nanoparticles prepared by green methods for heavy metal ions removal from water. *undefined* **178**, 744–751 (2013).

67. Liu, X., Hu, Q., Fang, Z., Zhang, X. & Zhang, B. Magnetic chitosan nanocomposites: a useful recyclable tool for heavy metal ion removal. *undefined* **25**, 3–8 (2009).

68. Song, J., Kong, H. & Jang, J. Adsorption of heavy metal ions from aqueous solution by polyrhodanine-encapsulated magnetic nanoparticles. *undefined* **359**, 505–511 (2011).

69. Behrens, S. Preparation of functional magnetic nanocomposites and hybrid materials: recent progress and future directions. *undefined* **3**, 877–892 (2011).

70. Liu, J., Wang, C. & Xiong, Z. Adsorption behavior of magnetic multiwalled carbon nanotubes for the simultaneous adsorption of furazolidone and Cu(II) from aqueous solutions. *Environ Eng Sci* **32**, 960–969 (2015).

71. Mubarak, N. M., Kundu, A., Sahu, J. N., Abdullah, E. C. & Jayakumar, N. S. Synthesis of palm oil empty fruit bunch magnetic pyrolytic char impregnating with FeCl3 by microwave heating technique. *Biomass Bioenergy* **61**, 265–275 (2014).

72. Cheng, J. *et al.* CNT@Fe3O4@C Coaxial Nanocables: One-Pot, Additive-Free Synthesis and Remarkable Lithium Storage Behavior. *Chemistry – A European Journal* **19**, 9866–9874 (2013).

73. Ren, L., Huang, S., Fan, W. & Liu, T. One-step preparation of hierarchical superparamagnetic iron oxide/graphene composites via hydrothermal method. *undefined* **258**, 1132–1138 (2011).

74. Reddy, D. H. K. & Yun, Y. S. Spinel ferrite magnetic adsorbents: Alternative future materials for water purification? *undefined* **315**, 90–111 (2016).

75. Valenzuela, R. Novel applications of ferrites. *Physics Research International* (2012) doi:10.1155/2012/591839.

76. Litsardakis, G., Manolakis, I., Serletis, C. & Efthimiadis, K. G. Effects of Gd substitution on the structural and magnetic properties of strontium hexaferrites. *undefined* **316**, 170–173 (2007).

77. Kefeni, K. K., Mamba, B. B. & Msagati, T. A. M. Application of spinel ferrite nanoparticles in water and wastewater treatment: A review. *Separation and Purification Technology* vol. 188 399–422 Preprint at https://doi.org/10.1016/j.seppur.2017.07.015 (2017).

78. Sivashankar, R., Sathya, A. B., Vasantharaj, K. & Sivasubramanian, V. Magnetic composite an environmental super adsorbent for dye sequestration – A review. *undefined* **1–2**, 36–49 (2014).

79. Giri, S. K., Das, N. N. & Pradhan, G. C. Synthesis and characterization of magnetite nanoparticles using waste iron ore tailings for adsorptive removal of dyes from aqueous solution. *undefined* **389**, 43–49 (2011).

80. Roonasi, P. & Nezhad, A. Y. A comparative study of a series of ferrite nanoparticles as heterogeneous catalysts for phenol removal at neutral pH. *Mater Chem Phys* **172**, 143–149 (2016).

81. Feng, X., Guo, H., Patel, K., Zhou, H. & Lou, X. High performance, recoverable Fe3O4ZnO nanoparticles for enhanced photocatalytic degradation of phenol. *Chemical Engineering Journal* **244**, 327–334 (2014).

82. Lata, S. & Samadder, S. R. Removal of arsenic from water using nano adsorbents and challenges: A review. *undefined* **166**, 387–406 (2016).

83. Ahmed, M. A., El-Katori, E. E. & Gharni, Z. H. Photocatalytic degradation of methylene blue dye using Fe2O3/TiO2 nanoparticles prepared by sol–gel method. *J Alloys Compd* **553**, 19–29 (2013).

84. Tu, Y. J., Chang, C. K., You, C. F. & Wang, S. L. Treatment of complex heavy metal wastewater using a multi-staged ferrite process. *J Hazard Mater* **209–210**, 379–384 (2012).

85. Tu, Y. J., You, C. F., Chang, C. K., Chan, T. S. & Li, S. H. XANES evidence of molybdenum adsorption onto novel fabricated nano-magnetic CuFe2O4. *Chemical Engineering Journal* **244**, 343–349 (2014).

86. Tu, Y. J., You, C. F., Chang, C. K., Wang, S. L. & Chan, T. S. Arsenate adsorption from water using a novel fabricated copper ferrite. *Chemical Engineering Journal* **198–199**, 440–448 (2012).

87. Kainz, Q. M. & Reiser, O. Polymer- and dendrimer-coated magnetic nanoparticles as versatile supports for catalysts, scavengers, and reagents. *Acc Chem Res* **47**, 667–677 (2014).

88. Baig, R. B. N. & Varma, R. S. Magnetically retrievable catalysts for organic synthesis. *Chem Commun (Camb)* **49**, 752–770 (2013).

89. Nasir Baig, R. B., Nadagouda, M. N. & Varma, R. S. Magnetically retrievable catalysts for asymmetric synthesis. *Coord Chem Rev* **287**, 137–156 (2015).

90. Gupta, V. K. *et al.* Nanoparticles as Adsorbent; A Positive Approach for Removal of Noxious Metal Ions: A Review. *undefined* **34**, 195–214 (2015).

91. Iakovleva, E. & Sillanpää, M. The use of low-cost adsorbents for wastewater purification in mining industries. *Environ Sci Pollut Res Int* **20**, 7878–7899 (2013).

92. Moeinpour, F., Alimoradi, A. & Kazemi, M. Efficient removal of Eriochrome black-T from aqueous solution using NiFe2O4 magnetic nanoparticles. *J Environ Health Sci Eng* **12**, 1–7 (2014).

93. Chella, S. *et al.* Solvothermal synthesis of MnFe2O4-graphene composite—Investigation of its adsorption and antimicrobial properties. *Appl Surf Sci* **327**, 27–36 (2015).

94. Mahdavian, A. R. & Mirrahimi, M. A. S. Efficient separation of heavy metal cations by anchoring polyacrylic acid on superparamagnetic magnetite nanoparticles through surface modification. *Chemical Engineering Journal* **159**, 264–271 (2010).

95. Kumar, S. *et al.* Graphene oxide-MnFe2O4 magnetic nanohybrids for efficient removal of lead and arsenic from water. *ACS Appl Mater Interfaces* **6**, 17426–17436 (2014).

96. Sigdel, A., Park, J., Kwak, H. & Park, P. K. Arsenic removal from aqueous solutions by adsorption onto hydrous iron oxide-impregnated alginate beads. *Journal of Industrial and Engineering Chemistry* **35**, 277–286 (2016).

97. Kurian, J. & Mathew, M. J. Structural, Magnetic and Mossbauer Studies of Magnesium Ferrite Nanoparticles Prepared by Hydrothermal Method. *Int J Nanosci* **17**, (2018).

98. Franco, A. & Silva, M. S. High temperature magnetic properties of magnesium ferrite nanoparticles. *J Appl Phys* **109**, (2011).

99. Reddy, D. H. K. & Yun, Y. S. Spinel ferrite magnetic adsorbents: Alternative future materials for water purification? *Coord Chem Rev* **315**, 90–111 (2016).

100. Kumar, S. & Kumar, A. Chemically derived luminescent graphene oxide nanosheets and its sunlight driven photocatalytic activity against methylene blue dye. *Opt Mater (Amst)* **62**, 320–327 (2016).

101. Kaur, N., Kaur, M. & Singh, D. Fabrication of mesoporous nanocomposite of graphene oxide with magnesium ferrite for efficient sequestration of Ni (II) and Pb (II) ions: Adsorption, thermodynamic and kinetic studies. *Environmental Pollution* **253**, 111–119 (2019).

102. Meidanchi, A. & Akhavan, O. Superparamagnetic zinc ferrite spinel–graphene nanostructures for fast wastewater purification. *Carbon N Y* **69**, 230–238 (2014).

103. Li, N. *et al.* Preparation of magnetic CoFe2O4-functionalized graphene sheets via a facile hydrothermal method and their adsorption properties. *J Solid State Chem* **184**, 953–958 (2011).

104. Kumar, S. & Kumar, A. Chemically derived luminescent graphene oxide nanosheets and its sunlight driven photocatalytic activity against methylene blue dye. *Opt Mater (Amst)* **62**, 320–327 (2016).

105. Kaur, M., Singh, M., Mukhopadhyay, S. S., Singh, D. & Gupta, M. Structural, magnetic and adsorptive properties of clay ferrite nanocomposite and its use for effective removal of Cr (VI) from water. *J Alloys Compd* **653**, 202–211 (2015).

106. Kaur, M., Kaur, N., Jeet, K. & Kaur, P. MgFe2O4 nanoparticles loaded on activated charcoal for effective removal of Cr (VI) – A novel approach. *Ceram Int* **41**, 13739–13750 (2015).

107. Ivanets, A. I. *et al.* Magnesium ferrite nanoparticles as a magnetic sorbent for the removal of Mn2+, Co2+, Ni2+ and Cu2+ from aqueous solution. *Ceram Int* **44**, 9097–9104 (2018).

108. Yahya, M. D., Obayomi, K. S., Abdulkadir, M. B., Iyaka, Y. A. & Olugbenga, A. G. Characterization of cobalt ferrite-supported activated carbon for removal of chromium and lead ions from tannery wastewater via adsorption equilibrium. *Water Science and Engineering* **13**, 202–213 (2020).

109. Taha, A. A., Moustafa, A. H. E., Abdel-Rahman, H. H. & Abd El-Hameed, M. M. A. Comparative biosorption study of Hg (II) using raw and chemically activated almond shell: *https://doi.org/10.1177/0263617417705473* **36**, 521–548 (2017).

110. William Kajjumba, G., Emik, S., Öngen, A., Kurtulus Özcan, H. & Aydın, S. Modelling of Adsorption Kinetic Processes—Errors, Theory and Application. in *Advanced Sorption Process Applications* (IntechOpen, 2019). doi:10.5772/intechopen.80495.

111. Srivastava, V., Sharma, Y. C. & Sillanpää, M. Application of nano-magnesso ferrite (n-MgFe 2 O 4) for the removal of Co 2+ ions from synthetic wastewater: Kinetic, equilibrium and thermodynamic studies. *Appl Surf Sci* **338**, 42–54 (2015).

112. Ayawei, N., Ebelegi, N. & Wankasi, D. Modelling and Interpretation of Adsorption Isotherms. (2017) doi:10.1155/2017/3039817.

113. Srivastava, V., Sharma, Y. C. & Sillanpää, M. Application of nano-magnesso ferrite (n-MgFe2O4) for the removal of Co2+ ions from synthetic wastewater: Kinetic, equilibrium and thermodynamic studies. *Appl Surf Sci* **338**, 42–54 (2015).

114. Hayes, T. L. & Pease, R. F. The scanning electron microscope: principles and applications in biology and medicine. *Adv Biol Med Phys* **12**, 85–137 (1968).

115. Dutta, A. Fourier Transform Infrared Spectroscopy. *Spectroscopic Methods for Nanomaterials Characterization* **2**, 73–93 (2017).

116. Raza Khan, S., Sharma, B., Chawla, P. A. & Bhatia, R. Inductively Coupled Plasma Optical Emission Spectrometry (ICP-OES): a Powerful Analytical Technique for Elemental Analysis. doi:10.1007/s12161-021-02148-4.

117. Kurian, M. *et al.* Structural, magnetic, and acidic properties of cobalt ferrite nanoparticles synthesised by wet chemical methods. *Journal of Advanced Ceramics* **2015**, 199–205.

118. Jung, K. W., Lee, S. Y. & Lee, Y. J. Facile one-pot hydrothermal synthesis of cubic spinel-type manganese ferrite/biochar composites for environmental remediation of heavy metals from aqueous solutions. *Bioresour Technol* **261**, 1–9 (2018).

119. Fato, F. P., Li, D. W., Zhao, L. J., Qiu, K. & Long, Y. T. Simultaneous Removal of Multiple Heavy Metal Ions from River Water Using Ultrafine Mesoporous Magnetite Nanoparticles. *ACS Omega* **4**, 7543–7549 (2019).